AD-A042 116 PACIFIC-SIERRA RESEARCH CORP SANTA MONICA CALIF F/G 9/3
ELF NOISE STATISTICS AND PROCESSING UNDER DISTURBED CONDITIONS.(U)
DEC 74 E C FIELD, R BERLOT N00014-74-C-0234
UNCLASSIFIED PSR-411 NL

1 OF 2
AD A042116

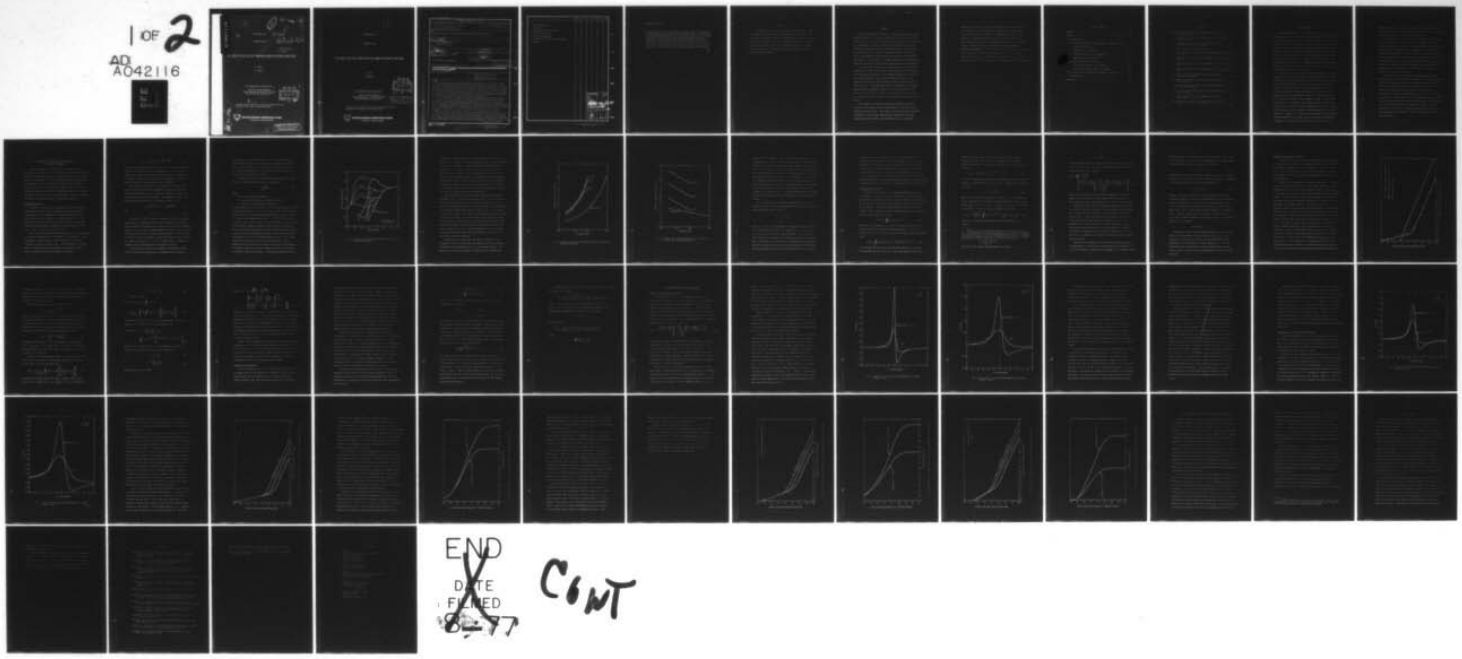

END
DATE FILMED
9-77

CONT

PSR REPORT 411

DECEMBER 1974

ELF NOISE STATISTICS AND PROCESSING UNDER DISTURBED CONDITIONS

E. Field

R. Berlot

This research was sponsored by:

Office of Naval Research
Under Contract No. N00014-74-C-0234,
NR 089-103/12-7-73, Code 464

PACIFIC·SIERRA RESEARCH CORP.
1456 Cloverfield Blvd. · Santa Monica, California 90404

(1)

PSR REPORT 411

DECEMBER 1974

ELF NOISE STATISTICS AND PROCESSING UNDER DISTURBED CONDITIONS

E. Field

R. Berlot

This research was sponsored by:

Office of Naval Research
Under Contract No. N00014-74-C-0234,
NR 089-103/12-7-73, Code 464

PACIFIC·SIERRA RESEARCH CORP.

1456 Cloverfield Blvd. · Santa Monica, California 90404

Unclassified
Security Classification

DOCUMENT CONTROL DATA - R & D

(Security classification of title, body of abstract and indexing annotation must be entered when the overall report is classified)

1. ORIGINATING ACTIVITY (Corporate author)

PACIFIC-SIERRA RESEARCH CORPORATION
1456 Cloverfield Boulevard
Santa Monica, California 90404

2a. REPORT SECURITY CLASSIFICATION: Unclassified

2b. GROUP

3. REPORT TITLE

ELF NOISE STATISTICS AND PROCESSING UNDER DISTURBED CONDITIONS

4. DESCRIPTIVE NOTES (Type of report and inclusive dates)

Final Report

5. AUTHOR(S) (First name, middle initial, last name)

E. C. Field, R. Berlot

6. REPORT DATE: December 1974

7a. TOTAL NO. OF PAGES: 53 (12 585)

7b. NO. OF REFS: 15

8a. CONTRACT OR GRANT NO: N00014-74-C-0234

8b. PROJECT NO: NR089-103/12-7-73 Code 464

8c.

8d.

9a. ORIGINATOR'S REPORT NUMBER(S): PSR Report-411

9b. OTHER REPORT NO(S) (Any other numbers that may be assigned this report)

DISTRIBUTION STATEMENT A
Approved for public release;
Distribution Unlimited

10. DISTRIBUTION STATEMENT

~~This document may be further distributed by any holder only with specific prior approval of ONR, Code 464.~~

11. SUPPLEMENTARY NOTES

12. SPONSORING MILITARY ACTIVITY
Office of Naval Research
Department of the Navy
Arlington, Virginia 22217

13. ABSTRACT

This report addresses the question of whether nonlinear processing schemes optimized on the basis of ambient extremely-low-frequency (ELF) atmospheric noise data will give near-optimum processing gain in nuclear/PCA environments. Analytic expressions are derived for noise-pulse waveforms, amplitude probability distributions (APDs), and processing gain as a function of clip levels. Numerical results are given for each of these quantities under ambient and spread-debris-nuclear/PCA environments. Good agreement is obtained with ambient ELF atmospheric noise data and results from much more complicated numerical treatments.

It is shown that, depending on certain definitions, noise-pulse durations can be three or four times longer in nuclear/PCA environments than under ambient conditions. This anomalous spreading is due mainly to increased attenuation in the earth-ionosphere waveguide, which selectively removes the highest-frequency Fourier components from the ELF noise pulse. The maximum degradation in processing gain caused by anomalous pulse spreading is found to be no greater than 1 or 2 dB. *Smearing of noise pulses in disturbed environments therefore does not pose a major problem to nonlinear noise suppression in ELF communication systems.*

The ionospheric disturbances considered significantly increase the ratio of the energy carried in noise spikes to the energy of the background Gaussian noise. This change in ratio, which alters the APDs considerably, occurs because Gaussian noise propagates over longer distances than noise spikes, and therefore tends to be suppressed relative to the spikes by increased attenuation. On the other hand,

(continued next page)

DD FORM 1 NOV 65 1473

407486

Unclassified
Security Classification

14 KEY WORDS	LINK A		LINK B		LINK C	
	ROLE	WT	ROLE	WT	ROLE	WT
ELF Communications						
ELF Noise						
Atmospheric Noise Statistics						
ELF Noise Processing						
ELF Pulse Propagation						
Communication in Nuclear Environments						
SANGUINE						

ABSTRACT (continued)

total RMS noise, to which noise spikes make the major contribution, may well be affected only slightly by environmental changes. Consequently, to achieve maximum processing gain, clip levels should be set according to the ratio of noise-spike energy to Gaussian background energy. Because this ratio can change drastically, an adaptive procedure is called for. *Calculations show that the experimental SANGUINE noise-suppression circuit, which self-adapts to clip some specified fraction--typically 20 to 60 percent--of the time gives nearly optimum processing gain for a wide variety of ambient and nuclear/PCA environments.*

PREFACE

This report gives results of one phase of Pacific-Sierra's study of long-wave atmospheric noise in certain nuclear environments. It addresses the question of whether nonlinear processing schemes optimized on the basis of ambient extremely-low-frequency (ELF) noise data will give near-optimum processing gain in nuclear environments. Another aspect of the study, not reported here, is concerned with very-low-frequency noise processing.

SUMMARY

This report addresses the question of whether nonlinear processing schemes optimized on the basis of ambient extremely-low-frequency (ELF) atmospheric noise data will give near-optimum processing gain in nuclear/PCA environments. Analytic expressions are derived for noise-pulse waveforms, amplitude probability distributions (APDs), and processing gain as a function of clip levels. Numerical results are given for each of these quantities under ambient and spread-debris-nuclear/PCA environments. Good agreement is obtained with ambient ELF atmospheric noise data and results from much more complicated numerical treatments.

It is shown that, depending on certain definitions, noise-pulse durations can be three or four times longer in nuclear/PCA environments than under ambient conditions. This anomalous spreading is due mainly to increased attenuation in the earth-ionosphere waveguide, which selectively removes the highest-frequency Fourier components from the ELF noise pulse. The maximum degradation in processing gain caused by anomalous pulse spreading is found to be no greater than 1 or 2 dB. *Smearing of noise pulses in disturbed environments therefore does not pose a major problem to nonlinear noise suppression in ELF communication systems.*

The ionospheric disturbances considered significantly increase the ratio of the energy carried in noise spikes to the energy of the background Gaussian noise. This change in ratio, which alters the APDs considerably, occurs because Gaussian noise propagates over longer distances than noise spikes, and therefore tends to be suppressed

relative to the spikes by increased attenuation. On the other hand, *total* RMS noise, to which noise spikes make the major contribution, may well be affected only slightly by envrionmental changes. Consequently, to achieve maximum processing gain, clip levels should be set according to the ratio of noise-spike energy to Gaussian background energy. Because this ratio can change drastically, an adaptive procedure is called for. *Calculations show that the experimental SANGUINE noise-suppression circuit, which self-adapts to clip some specified fraction--typically 20 to 60 percent--of the time gives nearly optimum processing gain for a wide variety of ambient and nuclear/PCA environments.*

TABLE OF CONTENTS

FIGURES

I. INTRODUCTION

Extremely-low-frequency (ELF) atmospheric noise consists of large pulses superimposed on a more homogeneous background. These pulses are due to nearby lightning flashes, whereas the background, which is nearly Gaussian, consists of many unresolved pulses from distant thunderstorm activity. Because most of the noise energy is typically contained in the noise spikes, which are present only a small fraction of the time, nonlinear circuit elements can be used to suppress most of the noise while only slightly degrading the signal. One such scheme that has proven successful is the use of a clipper, with the clipping level set just above the background noise peaks but well below the peaks of the large impulses (*Evans and Griffiths, 1974*).

A widespread ionospheric disturbance, such as would be caused by high-altitude nuclear detonations or a polar-cap absorption (PCA) event, can significantly change the manner in which ELF waves travel in the earth-ionosphere waveguide. Typically, attenuation is increased relative to ambient conditions, whereas phase velocity is reduced. Moreover, propagation becomes more dispersive. Because ELF noise propagates in the earth-ionosphere waveguide in much the same manner as a communication signal, these propagation changes can alter noise characteristics. Accordingly, this report addresses the question of whether nonlinear processing schemes optimized on the basis of ambient ELF noise data will give the maximum processing gain under disturbed conditions. Emphasis is on the statistical description and processing of ELF atmospheric noise, rather than on calculation of propagation anomalies in disturbed environments (which has received adequate

attention in the past). Thus, an idealized spread-debris/PCA model is used to describe the ionospheric disturbance, whence previously published results can be used for the propagation parameters.

An ionospheric disturbance can affect atmospheric noise characteristics in several ways. First, the anomalous attenuation tends to reduce the RMS noise. Second, and even more important, this attenuation alters the ratio of impulse noise to Gaussian noise, since these two components traverse paths of different lengths in propagating from the source lightning strokes to the receiver. This change in ratio significantly affects the noise amplitude probability distribution (APD). Finally, the anomalous dispersion associated with spread-debris/PCA environments can, in principle, cause noise-pulse durations to be longer than for ambient conditions.

Section II contains the mathematical development necessary to analyze the effects of nuclear/PCA environments. Previously published, relevant propagation calculations are reviewed, and mathematically tractable relations are derived for noise-pulse waveform, ELF noise probability density function (PDF) and APD, and processing gain achievable with clippers. These relations are in a form particularly convenient for assessing the effects of environmental changes. Section III gives numerical results for pulse waveforms, APDs, and processing gain under ambient and disturbed conditions. Section IV briefly discusses the possibility of increases in thunderstorm activity in the post-detonation environment. Section V presents the report's main conclusions.

II. STATISTICAL DESCRIPTION AND PROCESSING OF ATMOSPHERIC NOISE

This section presents the mathematical relationships used to obtain the results given in Sec. III. First, some results from previous reports on long-wave propagation in ambient and disturbed environments are briefly summarized. Second, closed-form expressions that describe the dispersion of ELF noise pulses under ambient and disturbed conditions are derived. Third, relatively simple representations of the probability density function (PDF) and amplitude probability distribution (APD) of ELF atmospheric noise are obtained. Finally, expressions are given for the processing gain achievable with clippers.

LONG-WAVE PROPAGATION

The theory of propagation of ELF waves in the earth-ionosphere waveguide has been the subject of numerous papers, and is generally well understood. For convenience, we summarize certain previously published results used as inputs to derivations given below. These results are taken mainly from the work of Field *(1969)*, although the reader desiring more detail is referred to other treatments as well (e.g., *Galejs, 1972; Wait, 1962; Budden, 1961).*

At ELF, only the quasi-TEM mode, which has no cutoff, can propagate in the earth-ionosphere cavity. The effects of the geomagnetic field on propagation can be neglected for the daytime and/or disturbed ionospheric conditions considered here. If the distance, r, from the source is greater than about one megameter, the vertical electric field, E_z, associated with the TEM mode can be written

$$E_z \approx A\omega^{1/2} r^{-1/2} S^{3/2} \Lambda\, e^{i\omega\left(t - \frac{rS}{c}\right)} , \qquad (1)$$

where ω is the angular frequency of the wave, Λ is the mode excitation factor, S is the sine of the mode eigenangle, and c is the speed of light. For a given source strength, the factor A may be regarded as a constant. Equation (1) applies only for monochromatic signals or a Fourier component of a signal having finite bandwidth.

The effects of the ionosphere on propagation are included in S, which is essentially the complex propagation constant for the earth-ionosphere waveguide, and in Λ. Both S and Λ depend on frequency as well as on the state of the ionosphere. The attenuation rate, α, and the relative phase velocity, c/v, are given in terms of S by

$$\alpha = 8.7 \times 10^{6} \frac{\omega}{c} Im\ S \qquad \text{dB/megameter} \qquad (2)$$

and

$$c/v = Re\ S \quad . \qquad (3)$$

The effect of either a natural or a man-made (nuclear) ionospheric disturbance is to alter the electron- and ion-density height profiles, thereby changing the propagation characteristics of the earth-ionosphere waveguide. In the case of a high-altitude nuclear burst, x-rays, γ-rays, and beta particles create ion pairs in the atmosphere, a large fraction of which are below the altitudes at which ELF reflection usually occurs. In a polar-cap absorption (PCA) event, a similar effect is caused by energetic protons impinging upon the ionosphere from above.

To illustrate the effect that ionospheric disturbances can have on noise statistics and processing, we consider an easily analyzed

type of nuclear environment; namely, one in which fission debris is spread fairly uniformly over a large area at altitudes above 100 km or so. Although other types of environments could certainly occur and produce effects numerically different from those given here, the spread-debris model serves our purposes.

A convenient parameter to characterize the spread-debris environment is the ionizing intensity factor, Γ, defined as

$$\Gamma = \frac{(FY)}{R^2 t^{1.2}} \quad , \tag{4}$$

where

FY = total fission yield (megatons),

R = radius over which debris is spread (kilometers),

t = time after debris deposition (seconds).

By using methods discussed by Crain *(1964)*, the quasi-equilibrium ionization-balance equations (e.g., *Fisher and Knapp, 1967)* can be solved to obtain electron- and ion-density height profiles for various values of Γ. Figure 1 shows computed profiles for $\Gamma = 10^{-12}$, 10^{-10}, and 10^{-8}--a reasonable range of values--along with nominal ambient daytime profiles. To obtain mode propagation parameters, these profiles must first be used in conjunction with electron- and ion-collision-frequency profiles to obtain refractive-index height profiles. Then, various procedures are available to solve the well-known modal equation for S and, hence, attenuation, phase velocity, and the excitation factor. Here, a numerical full-wave method that accounts for the vertical inhomogeneity in refractive index has been used to obtain α and v/c for the ionization height profiles shown in Fig. 1. The method (essentially that of

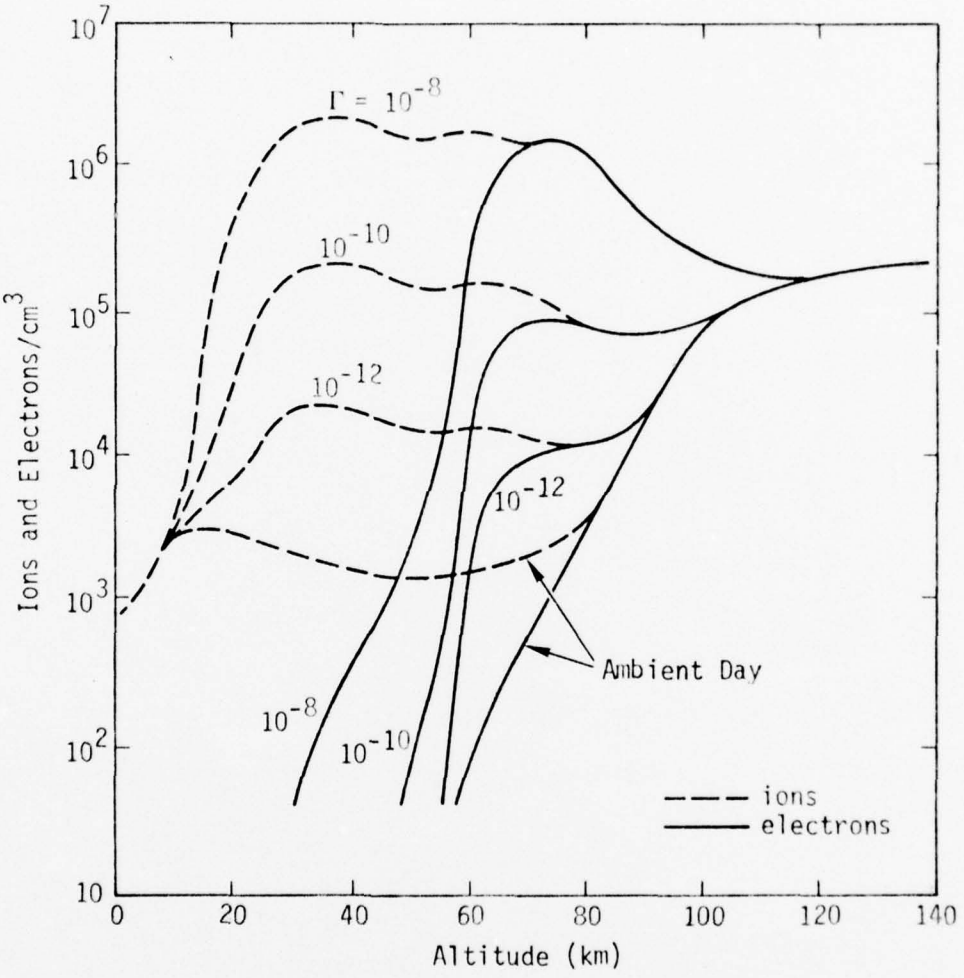

Fig. 1--Daytime ionization height profiles for ambient and disturbed conditions

Budden) and its application are described in detail by Field (1969). Figures 2 and 3 show the calculated attenuation rates and phase velocities as functions of frequency. Comparison between the ionization profiles shown in Fig. 1 and analogous ones derived by Field (1969) for PCA events indicates a similarity between spread-debris environments and those associated with strong PCAs. It is therefore not surprising that the values of α and c/v shown in Figs. 2 and 3 are similar in magnitude to those calculated by Field (1969) for certain PCA events. Thus, to a first approximation, the results given below are applicable to strong PCA as well as spread-debris nuclear environments.

Three main effects caused by disturbed environments are evident from Figs. 2 and 3. First, the attenuation rate is increased over the ambient value although, for the cases shown, the magnitude of the increase is surprisingly insensitive to the strength of the disturbance. At the currently interesting frequency of about 50 Hz, α is calculated to be about 0.8 dB/Mm (in good agreement with measurements) under ambient conditions and in the 1.5- to 2-dB/Mm range for the disturbed environments considered. Second, phase velocity decreases significantly under disturbed conditions, and is considerably (>20 percent) less than the speed of light for all cases. Third, propagation is much more dispersive under disturbed than under ambient conditions; i.e., α and c/v vary more strongly with frequency.

Calculations not reported here show that, in addition to the propagation effects just described, spread-debris or PCA environments generally cause the excitation factor, A, to increase somewhat. The magnitude of the increase depends on various factors, including the

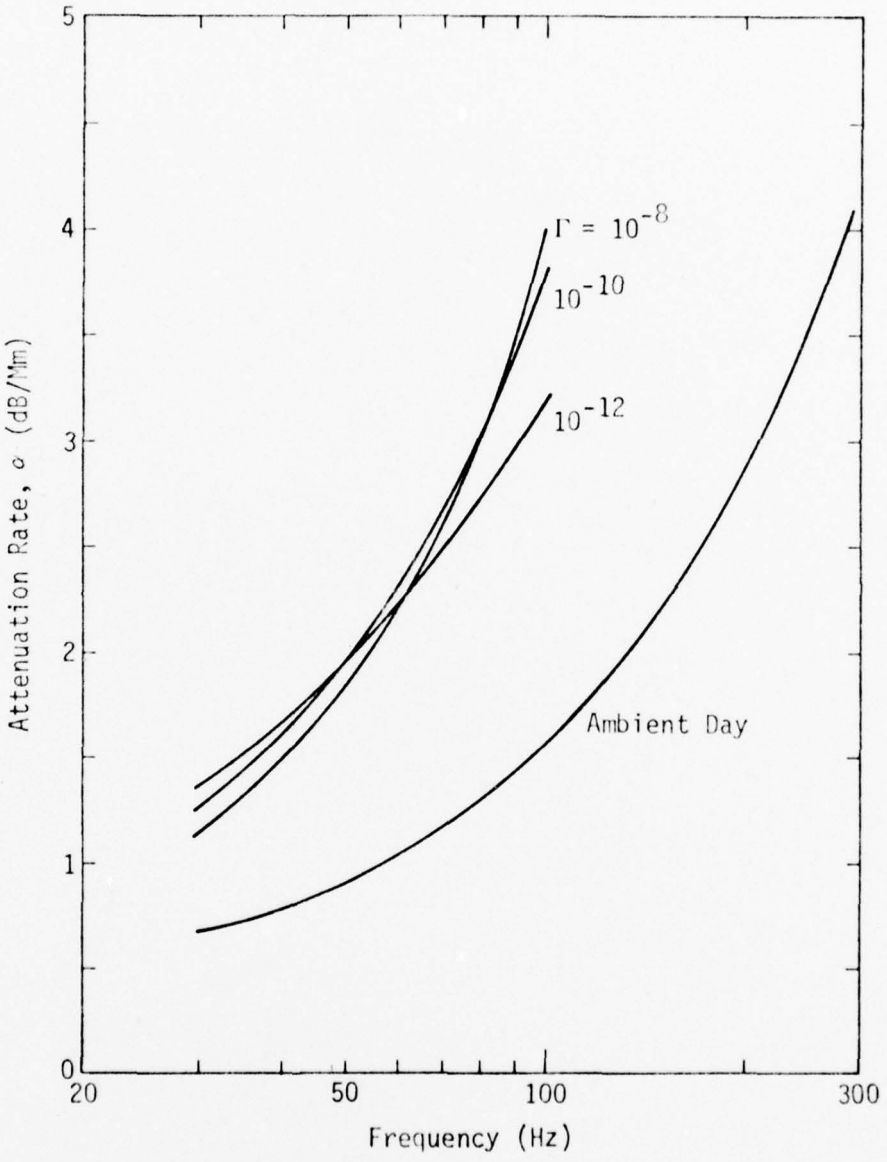

Fig. 2--Computed ELF daytime attenuation rates for ambient and disturbed conditions

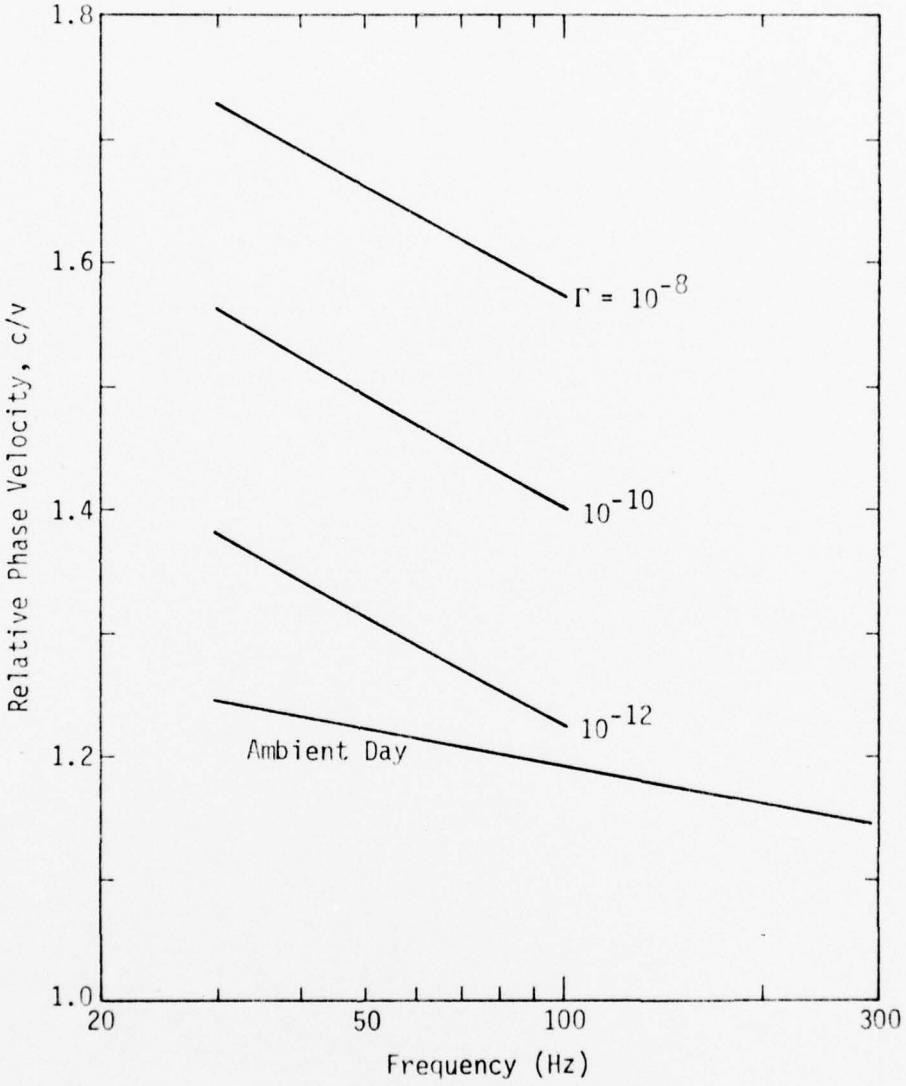

Fig. 3--Computed ELF daytime relative phase velocities for ambient and disturbed conditions

location of the disturbance relative to both source and receiver. If a disturbance were confined to the center portion of a propagation path and did not extend to the source and receiver regions, no increase in A would occur. However, an increase as large as 6 or 8 dB could occur if both source and receiver locations were affected strongly. A good working assumption is that an increase of a few decibels in A will occur. For propagation paths shorter than, say, 2 or 3 Mm, the magnitude of the excitation enhancement equals or exceeds the degradation in propagation, and little change (perhaps a slight increase) is noted in the strength of the signal received. For longer paths, propagation degradation typically dominates excitation enhancement, and a net signal loss results.

It is convenient to use an analytic approximation to S in the following analysis. One such approximation that is simple and accurate over the frequency band of interest is

$$Re\ S \simeq S_0 + S_1/\omega \qquad (5)$$

$$Im\ S \simeq S_i \quad , \qquad (6)$$

where S_0, S_1, and S_i are independent of frequency and may be found by fitting the numerical results. For example, for $\Gamma = 10^{-8}$, $S_0 = 1.51$, $S_1 = 42.7$, and $S_i = 0.2$ fit the results of Figs. 2 and 3 to within about 10 percent for frequencies between a few tens and a few hundred Hertz. The analytic fits given by Eqs. (5) and (6) become invalid for ultra-low frequencies ($\lesssim$10 Hz) and very low frequencies ($\gtrsim$1 kHz) and, strictly speaking, should be used only within the ELF band. In fact,

inaccuracies in S at frequencies above a few hundred Hertz do not greatly affect the precision of the calculations since waves at these frequencies are highly attenuated and contribute relatively little to the total field. Moreover, SANGUINE receiver filters will probably have an upper cutoff of no higher than a few hundred Hertz (*Griffiths, 1972*). The practical limit is thus the lower one (about 10 Hz) in the frequency domain or, for pulse propagation calculations in the time domain, the approximation becomes invalid for times greater than 50 to 100 msec.

DISPERSION OF ELF PULSES

In general, the response of the earth-ionosphere waveguide to a time-varying source must be computed numerically. However, by using the equations and approximations given above, a simple analytic expression can be derived that describes pulse spreading with sufficient accuracy for our purposes. We begin by noting that, in the time domain, the electric field at a distance r from a vertically polarized source having arbitrary time dependence is given by

$$E(t,r) = \int_{-\infty}^{\infty} d\omega g(\omega) T(\omega,r)\ e^{i\omega t} \quad , \tag{7}$$

where $g(\omega)$ is the frequency spectrum of the source and $T(\omega,r)$ is the transfer function of the earth-ionosphere waveguide. Since $E(t,r)$ must be real, Eq. (7) can be rewritten in the following, more convenient, form:

$$E(t,r) = \int_{0}^{\infty} d\omega\ [g(\omega)T(\omega)\ e^{i\omega t} + g^*(\omega)T^*(\omega)\ e^{-i\omega t}] \quad . \tag{8}$$

It is assumed that the source is an impulse, whence $g(\omega)$ = constant. This approximation works well for ELF and ranges greater than several

hundred kilometers, where pulse duration exceeds source duration. Results given below agree well with the results of more detailed numerical treatments. Moreover, from Eq. (1), the transfer function is given by

$$T(\omega,r) = AS^{3/2}A\omega^{1/2}r^{-1/2}\, e^{-\frac{|\omega|}{c}r\,Im S}\, e^{-i\frac{\omega}{c}r\,Re S} \quad . \tag{9}$$

It is now convenient to approximate the three-term product $AS^{3/2}A$ that appears as a multiplicative factor in Eq. (9). Specifically, we use the fact that

$$AA \simeq |AA|\, e^{\pi i/4} \quad , \tag{10}$$

where $|AA|$ can be assumed independent of ω and $S \simeq S_o$.† Note that the latter approximation is used only in the multiplicative factor, but not in the exponent, where the entire expressions given by Eqs. (5) and (6) are retained. Thus, for an impulse source, Eq. (8) becomes

$$E(t,r) \simeq \frac{2|AA|S_o^{3/2}}{r^{1/2}} \int_0^\infty d\omega\, \omega^{1/2}\, e^{-\frac{\omega}{c}rS_i} \cos\left(\frac{\pi}{4} - \frac{r}{c}S_1 + \omega\tau\right) \quad , \tag{11}$$

where Eqs. (5) and (6) have been used and the retarded time, τ, is given by

---

†The validity of the approximation $S \simeq S_o$ is clear from Eqs. (5) and (6). The approximation given in Eq. (10) stems from a numerical solution, but can be seen from an idealized treatment where the earth and ionosphere are modeled as sharply bounded layers separated by a distance h. In this case, it can be shown analytically (*Wait, 1962*, p. 292) that

$$AA = \frac{60\pi}{\sqrt{2\pi c}}\,\frac{Id\ell}{h}\, e^{\pi i/4} \quad ,$$

where $Id\ell$ is the electric dipole moment of the source.

$$\tau = t - \frac{rS_o}{c} \quad .$$

This approximation allows the integration to be evaluated analytically (*Erdélyi, 1954*, p. 14). After some rearrangement, the expression for the pulse waveform may be written

$$E(t,r) \sim \sqrt{\frac{\pi}{2}} \frac{S_o^{3/2}|AA|}{r^{1/2}} \cdot \left[\frac{\cos\left(\frac{3}{2}\,\text{Arctan}\left[\frac{c\tau}{rS_i}\right] - \frac{S_1 r}{c}\right) - \sin\left(\frac{3}{2}\,\text{Arctan}\left[\frac{c\tau}{rS_i}\right] - \frac{S_1 r}{c}\right)}{\left(\tau^2 + \frac{r^2 S_i^2}{c^2}\right)^{3/4}} \right] . \quad (12)$$

Since we are concerned only with the time dependence of E(t,r) and numerical results are given in normalized form, the magnitudes of the factors outside the square brackets in Eq. (12) are not of concern.

Equation (12) indicates that the pulse width depends mainly on S_i, i.e., on the severity of attenuation in the earth-ionosphere waveguide. Specifically, since the denominator of Eq. (12) begins to increase strongly when $\tau \geq rS_i/c$, pulse width is more or less proportional to the propagation path length and to the slope ($d\alpha/d\omega \propto S_i$) of the attenuation rate. This behavior is physically reasonable, since the broadening is mainly caused by the fact that propagation attenuates high-frequency components more strongly than low-frequency ones. The product rS_i is a measure of the degree to which this selective attenuation has occurred.

Equation (12) describes the ELF field from an impulse source as it would appear to a receiver having an infinitely wide bandwidth. It is also of interest to examine the time dependence of a lightning-induced

noise pulse after it has passed through a low-pass filter with an upper cutoff frequency, f_o. A heuristic model adequate for our purpose assumes a receiver having a frequency response, $F(\omega)$, given by

$$F(\omega) = e^{-B|\omega|} \quad . \tag{13}$$

Note that when the waveguide transfer function, $T(\omega,r)$ (see Eq. (9)) is multiplied by $F(\omega)$ to obtain the total transfer function, the ω-dependence is formally unchanged, provided that the transformation

$$\frac{rS_i}{c} \rightarrow B + \frac{rS_i}{c} \tag{14}$$

is made. This formal similarity is not surprising since the earth-ionosphere waveguide is itself a low-pass filter with a cutoff frequency inversely proportional to the length of the propagation path. When $B > rS_i/c$, the pulse width is governed mainly by the receiver filter, whereas when $rS_i/c > B$, the earth-ionosphere waveguide is the dominant factor. Numerical results are given in terms of a cutoff frequency, f_o, at which receiver response is 6 dB below its value at zero frequency. In terms of this frequency

$$B = 0.11/f_o \quad .$$

Finally, note that the approximations leading to Eq. (12) are non-casual, as is the assumed receiver filter (Eq. (13)), which is non-realizable. The main error caused by the non-realizability of the approximations is the presence of a small precursor for $\tau < 0$. The calculated effect of the environment on pulse width should be sufficiently accurate to assess the expected performance of nonlinear noise processors.

AMPLITUDE PROBABILITY DISTRIBUTION

To assess the effects of ionospheric disturbances on the performance of noise-processing techniques, a tractable expression for the APD of low-frequency atmospheric noise must be derived. In addition to accurately fitting noise data, this expression should explicitly contain the dependence of the APD on calculable propagation parameters, e.g., attenuation rate.

Observation of wideband ELF noise reveals large pulses superimposed upon a more homogeneous background. These pulses are caused by local thunderstorm activity, whereas the background is due to a large number of relatively weak unresolved pulses from more numerous distant lightning flashes. It follows from the central limit theorem that the low-level background should closely resemble Gaussian noise. However, at larger amplitudes, considerable departures from Gaussian noise are to be expected. Figure 4 shows the probability (or percent of time) that the absolute value of the recorded noise exceeds a given level in RMS units. For comparison, the APD of pure Gaussian noise is also shown. The small squares represent data taken during high-level noise at Saipan *(Modestino, 1971)*. The change in slope at around 1 percent (or, equivalently, at around -5 dB/RMS) represents a change from Gaussian to non-Gaussian statistics. Thus, about 99 percent of the time, the noise is Gaussian and is due to numerous distant thunderstorms; whereas about 1 percent of the time it is due mainly to infrequent, but strong, pulses from local activity. As is evidenced by the sharp increase in the APD at large amplitudes, the occurrence of intense noise is much more likely (i.e., it occurs much more often) than would be predicted on the basis

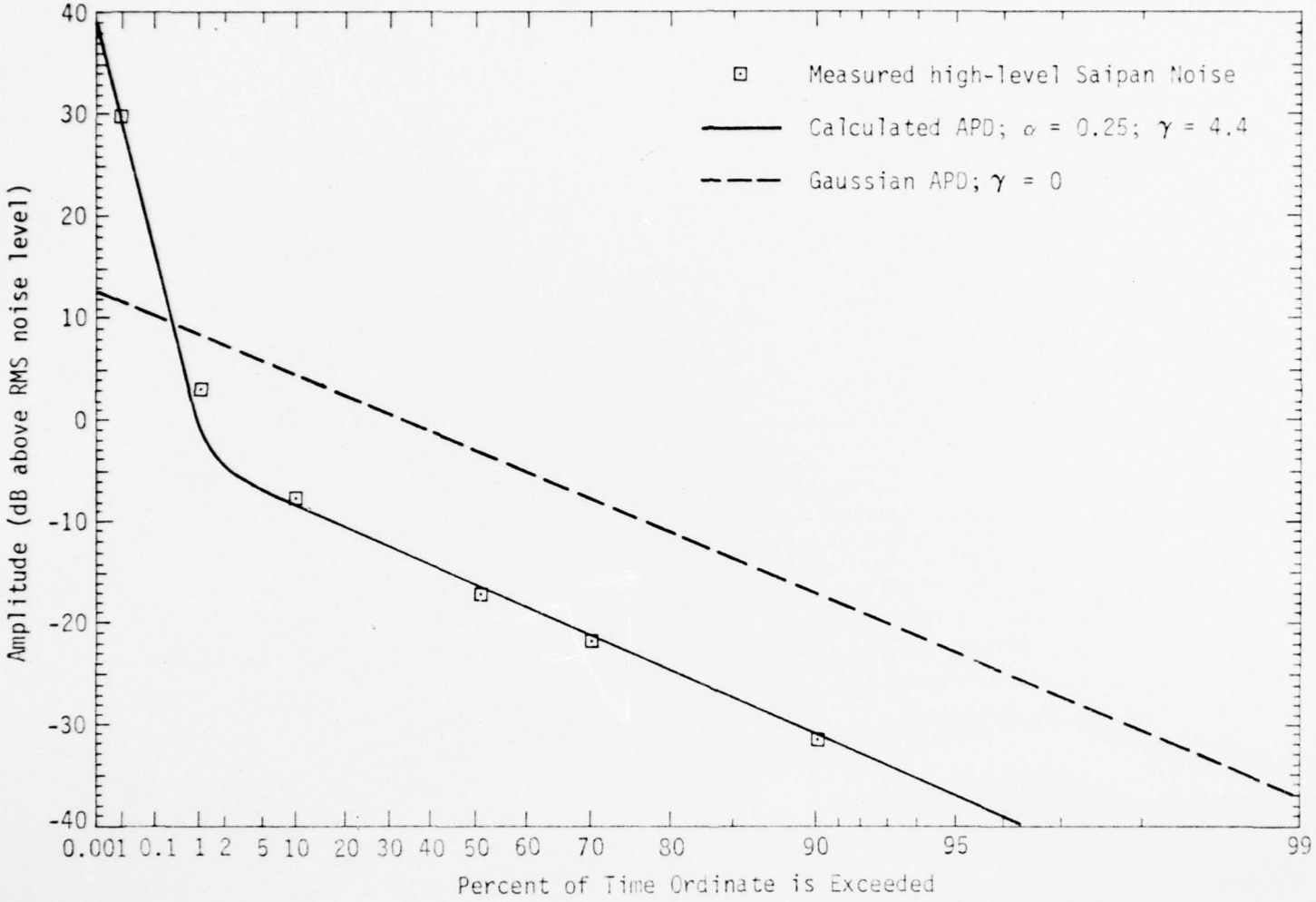

Fig. 4--APD of high-level Saipan ELF noise

of Gaussian statistics. Of course, Fig. 4 applies only to high-level Saipan noise. For different locations and noise conditions, the general characteristics of the APD are as shown in Fig. 4, although numerical magnitudes can be quite different.

The PDF of the Gaussian component of the noise is

$$f_1(x) = \frac{1}{\sqrt{2\pi}\,\sigma_o} e^{-x^2/2\sigma_o^2} , \qquad (15)$$

which, of course, has a variance of σ_o^2. For the non-Gaussian, spikey component, the PDF should allow for the relatively frequent occurrence of large amplitudes; i.e., the tails of this PDF should fall off much more slowly than for a Gaussian density function. Several choices are possible, but the double-sided Rayleigh distribution defined by

$$f_2(y) = \frac{\alpha |y|^{\alpha-1}}{2R_o^\alpha} \exp\left\{-\left|\frac{y}{R_o}\right|^\alpha\right\} \qquad (16)$$

and suggested by Modestino *(1971)* is convenient for analysis and is used. The variance of this function (i.e., the RMS noise of the non-Gaussian component) is $R_o^2\Gamma(1+\frac{2}{\alpha})$, where Γ is the gamma function and α is chosen to fit noise data.

The PDF of the total atmospheric noise (i.e., the PDF of the variable $z = x+y$) is obtained by convoluting the functions given by Eqs. (15) and (16). The resulting expression is

$$f(z) = \frac{\alpha}{2\sqrt{2\pi}\,R_o^\alpha \sigma_o} \int_{-\infty}^{\infty} dy |y|^{\alpha-1} \exp\left\{-\left[\frac{(z-y)^2}{2\sigma_o^2} + \left|\frac{y}{R_o}\right|^\alpha\right]\right\} , \qquad (17)$$

which must be evaluated numerically unless α assumes integer values, which is not the typical case. The variance, σ^2, of $f(z)$ is given by

$$\sigma^2 = \sigma_o^2 + R_o^2 \Gamma\left(1 + \frac{2}{\alpha}\right) \quad . \tag{18}$$

The APD is given by

$$\text{APD} = \text{Prob}(|z| > z_T) = 2 \int_{z_T}^{\infty} f(z)\, dz$$

$$= \frac{\alpha}{\sqrt{2\pi}\, R_o^{\alpha} \sigma_o} \int_{-\infty}^{\infty} dy \int_{z_T}^{\infty} dz\, |y|^{\alpha-1} \exp\left\{-\left[\frac{(z-y)^2}{2\sigma_o^2} + \left|\frac{y}{R_o}\right|^{\alpha}\right]\right\} \quad . \tag{19}$$

By performing the z-integration, and then integrating by parts with respect to y, it follows after some rearrangement that

$$\text{Prob}(|z| > z_T) = 1 - \text{erf}\left(\frac{z_T}{\sqrt{2}\,\sigma_o}\right) - \frac{1}{\sqrt{2\pi}\,\sigma_o}$$

$$\cdot \int_0^{\infty} dy\, e^{-(y/R_o)^{\alpha}} \left[e^{-(z_T+y)^2/2\sigma_o^2} - e^{-(z_T-y)^2/2\sigma_o^2}\right], \tag{20}$$

where erf is the error function. It is convenient to normalize the results to total RMS noise. Accordingly, substituting

$$\zeta_T = \frac{z_T}{\sigma} \tag{21}$$

and

$$\gamma^2 = \frac{R_o^2 \Gamma\left(1 + \frac{2}{\alpha}\right)}{\sigma_o^2} \tag{22}$$

into Eq. (20), it follows that

$$\text{Prob}(|\zeta|>\zeta_T) = 1 - \text{erf}\left(\frac{\sqrt{1+\gamma^2}}{\sqrt{2}}\,\zeta_T\right) - \frac{\sqrt{1+\gamma^2}}{2\pi}$$

$$\cdot \int_0^\infty d\eta\, \exp\left\{-\left[\eta^2\left(1+\frac{1}{\gamma^2}\right)\Gamma\left(1+\frac{2}{\alpha}\right)\right]^{\alpha/2}\right\}$$

$$\cdot \left\{\exp\left[-\left(\frac{1+\gamma^2}{2}\,(\zeta_T+\eta)^2\right)\right] - \exp\left[-\left(\frac{1+\gamma^2}{2}\,(\zeta_T-\eta)^2\right)\right]\right\} . \quad (23)$$

Equation (23), which is the basis of Pacific-Sierra's noise model, has some very convenient features. First, it involves only a single definite integral that is--and has been--easily programmed. Second, the APD is expressed in terms of only two parameters, α and γ^2, which for ambient conditions can be determined by comparison with data. Third, the effects of anomalous attenuation in disturbed environments are contained in γ^2, which is simply the ratio of RMS noise from nearby lightning activity to that from remote activity.

Figure 4 shows an example of how closely the theoretical APD fits ELF noise data. The solid line depicts the APD calculated from Eq. (23) for $\alpha = 0.25$ and $\gamma = 4.4$. These values were selected to provide a good fit to the data for the location and noise conditions indicated. It is seen that, by properly selecting only two parameters, an excellent representation of ELF noise statistics can be obtained.

NONLINEAR NOISE PROCESSING

For the case shown in Fig. 4, $\gamma^2 = 19.4$ (13 dB), which shows that the energy content of the spikey noise component is nearly a factor of twenty greater than the energy content of the Gaussian component. Stated differently, for high-level Saipan noise, about 95 percent of

the total RMS energy is due to large pulses from nearby thunderstorms. Also note from the shape of the APD in Fig. 4 that these noise spikes are present only a small fraction of the time. Thus, a nonlinear device that removes intense spikes could suppress most of the noise while only slightly degrading any signal that might be present. For example, a properly adjusted clipper could remove the majority of the noise while remaining in the linear regime much of the time. For these reasons, nonlinear ELF noise-processing schemes involving clippers, limiters, and hole punchers have been developed as part of the SANGUINE program (*Evans and Griffiths, 1974*). The effectiveness of the nonlinear processing was relatively insensitive to the details of the type of nonlinearity employed. Here, we only examine clipper performance.

To assess the effectiveness of clipping in a variety of noise environments, it is necessary to derive an expression for the processing gain in terms of the clip level, z_c, and the ratio, γ^2, of the non-Gaussian to Gaussian noise. Strictly speaking, the effective atmospheric noise (i.e., the post-processing RMS noise) depends somewhat on signal strength as well as on noise characteristics. The derivation given below neglects this dependence on signal strength, and the resulting "processing gain" is in fact more accurately described as a noise-suppression factor. This factor closely approximates the processing gain when the ratio of signal to total RMS noise is small.

To estimate the processing gain, PG, we use the following heuristic expression that accounts for the fact that no advantage is gained by clipping the noise to below the Gaussian background level; i.e., the maximum gain is achieved once the noise pulses from nearby thunderstorms are suppressed:

$$PG = \frac{\sigma_o^2 + R_o^2\Gamma(1 + \frac{2}{\alpha})}{\sigma_o^2 + \int_{-\infty}^{\infty} dz z^2 F^2(z, z_c) f_2(z)} \quad , \tag{24}$$

where f_2 is the Rayleigh distribution (Eq. (16)) and $F(z_c)$ is the clipping function, given by

$$F(z_c) = 1 \qquad |z| < z_c$$

$$= z_c/z \quad , \qquad |z| > z_c \quad .$$

The numerator of Eq. (24) is simply the sum, σ^2, of the RMS values of the Gaussian and non-Gaussian noise components. The first term in the denominator is RMS Gaussian noise, whereas the second term is RMS non-Gaussian noise after suppression by the clipper. As the clip level, z_c, approaches infinity, the second term in the denominator becomes $R_o^2\Gamma(1 + \frac{2}{\alpha})$ and PG → 1, indicating no processing gain. For very small clip levels, this term tends toward zero and

$$PG \xrightarrow[z_c = 0]{} \frac{\sigma_o^2 + R_o^2\Gamma(1 + \frac{2}{\alpha})}{\sigma_o^2} = 1 + \gamma^2 \quad , \tag{25}$$

which shows that, if all the close-in noise spikes are removed, the noise is suppressed by a factor $1+\gamma^2$; i.e., by the ratio of total noise to Gaussian noise. Of course, Eqs. (24) and (25) are not rigorously correct, since a clip level of zero would actually suppress *all* the noise *and* signal. However, these equations are an accurate representation when the clip level is set below the level of most of the strong noise spikes, but at or somewhat above the level of the RMS Gaussian noise from distant sources.

By inserting Eq. (16) into Eq. (24), the integral may be evaluated in closed form to obtain

$$PG \approx \frac{\sigma_o^2 + R_o^2\Gamma(1+\frac{2}{\alpha})}{\sigma_o^2 + R_o^2\Gamma(1+\frac{2}{\alpha})P\left[2(z_c/R_o)^\alpha \middle| 2+\frac{4}{\alpha}\right] + z_c^2 \exp[-(z_c/R_o)^\alpha]} \quad , \tag{26}$$

where $P(\chi^2|v)$ is the chi-square probability function (*Abramowitz and Stegun, 1964*). It is convenient to normalize the clipping level to RMS units and to express PG in terms of γ^2. Thus, using

$$\zeta_c = z_c/\sigma \quad ,$$

it follows that

$$PG = \frac{1+\gamma^2}{1+\gamma^2 P\left[2(\Omega\zeta_c)^\alpha \middle| 2+\frac{4}{\alpha}\right] + (1+\gamma^2)\zeta_c^2 \exp[-(\Omega\zeta_c)^\alpha]} \quad , \tag{27}$$

where

$$\Omega = \frac{\sqrt{1+\gamma^2}}{\gamma}\left(\Gamma(1+\frac{2}{\alpha})\right)^{1/2} \quad .$$

III. NUMERICAL RESULTS AND DISCUSSION

EFFECTS OF ANOMALOUS PULSE SPREADING

To illustrate the effects of nuclear/PCA environments on the dispersion of noise pulses, Eq. (12) has been used to calculate pulse waveforms for the assumed ambient environment ($\Gamma = 0$) and the most intense of the assumed nuclear environments ($\Gamma = 10^{-8}$). Our main interest is in the anomalous spreading caused by the ionospheric disturbance; i.e., we are more concerned with the time dependence of the pulse than with its magnitude. Thus, we give results for the normalized field, $\tilde{E}(r,\tau)$, given by (see Eq. (12))

$$\tilde{E}(r,\tau) = \frac{\cos\left(\frac{3}{2}\,\mathrm{Arctan}\left(\frac{c\tau}{rS_i}\right) - \frac{S_1 r}{c}\right) - \sin\left(\frac{3}{2}\,\mathrm{Arctan}\left(\frac{c\tau}{rS_i}\right) - \frac{S_1 r}{c}\right)}{\left(\tau^2 + \frac{r^2 S_i^2}{c^2}\right)^{3/4}} \quad , \qquad (28)$$

which fully describes the pulse waveform. For convenience in making comparisons, the results are plotted so that $\tilde{E}$ has a peak value of unity for ambient conditions, r = 1 Mm, and B = 0 (i.e., $f_o = \infty$--see Eq. (14)). Differences in excitation between ambient and disturbed conditions are therefore neglected. These differences affect relative peak amplitudes somewhat, but do not affect relative time spreading, which results solely from propagation.

From Eq. (28) it is seen that, in terms of the retarded time, τ, pulse shape is determined entirely by S_1, S_i, and--making the substitution indicated by Eq. (14)--by the receiver cutoff frequency, f_o. The values of S_1 and S_i that best fit the numerical results shown in Figs. 2 and 3 are $S_1 = 19.1$ and $S_i = 0.09$ for ambient conditions ($\Gamma = 0$),

and $S_l = 42.7$ and $S_i = 0.2$ for $\Gamma = 10^{-8}$. At ELF, the pre-processing bandwidth must be much wider than the information bandwidth lest the noise pulse be smeared so badly that it seriously degrades the processing gain achievable by clipping. For an ELF system having a center frequency that lies between 50 and 100 Hz, it has been shown (*Griffiths, 1972*) that upper cutoff frequencies at least as large as 150 to 200 Hz should be used. Accordingly, we give results for $f_o = \infty$ and $f_o = 300$ Hz.

Figures 5 and 6 show $\bar{E}$ versus time for ambient and disturbed environments, $f_o = \infty$, and distances from the source of 1 and 3 Mm. In the context of this report, distances greater than 3 Mm are not of interest since lightning at these large distances tends to contribute to the Gaussian rather than the Rayleigh (spikey) noise component, and would thus not be subjected to significant clipping.

In comparing the various cases, recall that all results shown are normalized so that the pulse labeled "ambient" on Fig. 5 has a peak amplitude of unity. Of course, it is difficult to uniquely define a pulse length, since this length depends upon certain arbitrary definitions of a pulse's "beginning" and "end." However, if one defines pulse length as the time during which the amplitude exceeds some reasonable threshold--say, 10 percent or so of the peak value--then for ambient conditions the calculated duration, τ_o, is about 3 msec for r = 1 Mm and 6 msec for r = 3 Mm. These values agree reasonably well with the 3- to 8-msec pulse widths measured for a variety of conditions and reported by Modestino *(1971)*. Moreover, aside from an unimportant difference in sign, the waveforms calculated here closely agree with those computed from a much more detailed numerical treatment and reported by Jones *(1970)*.

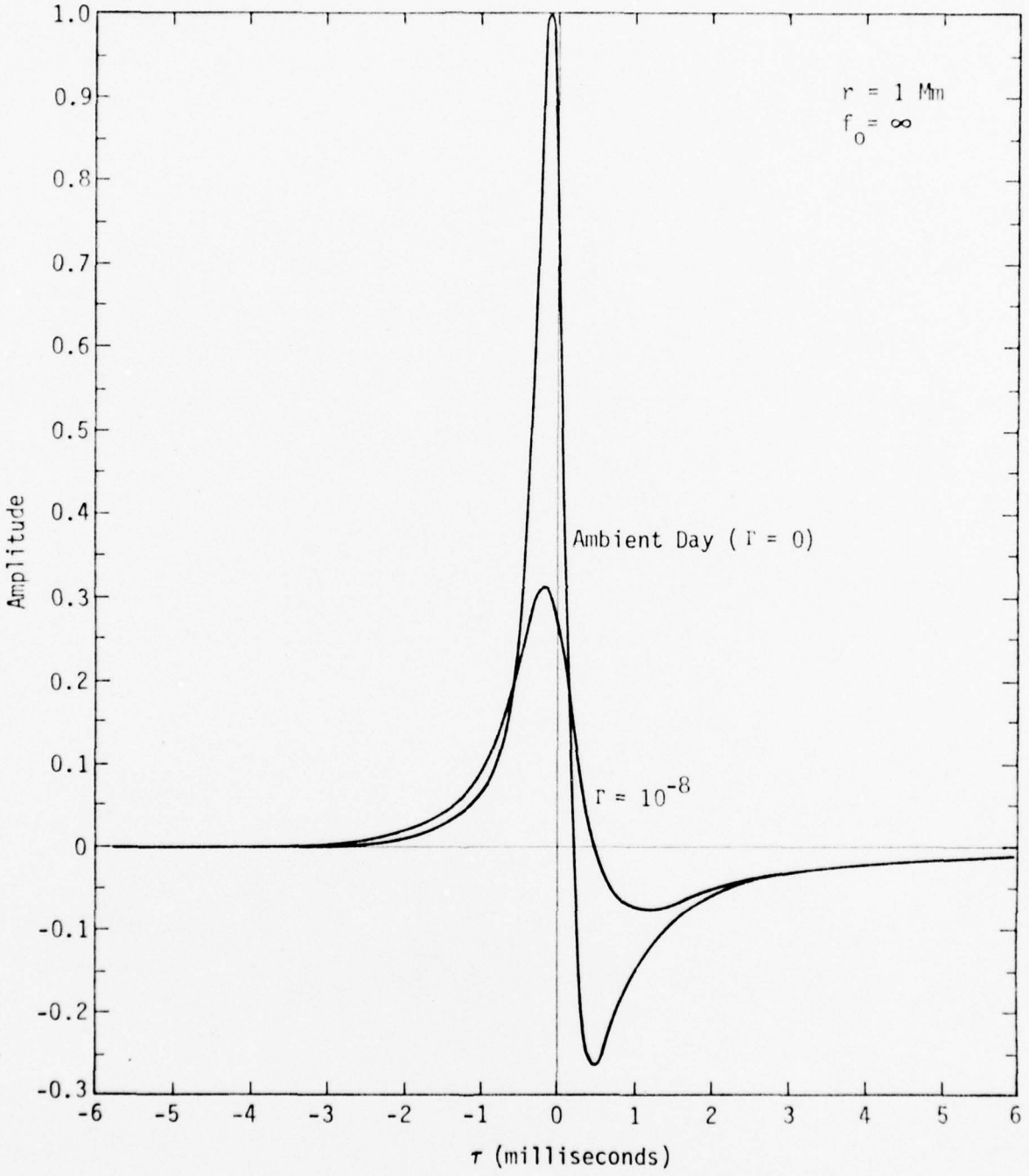

Fig. 5--Calculated ELF electric-field waveform for impulse source: Case A

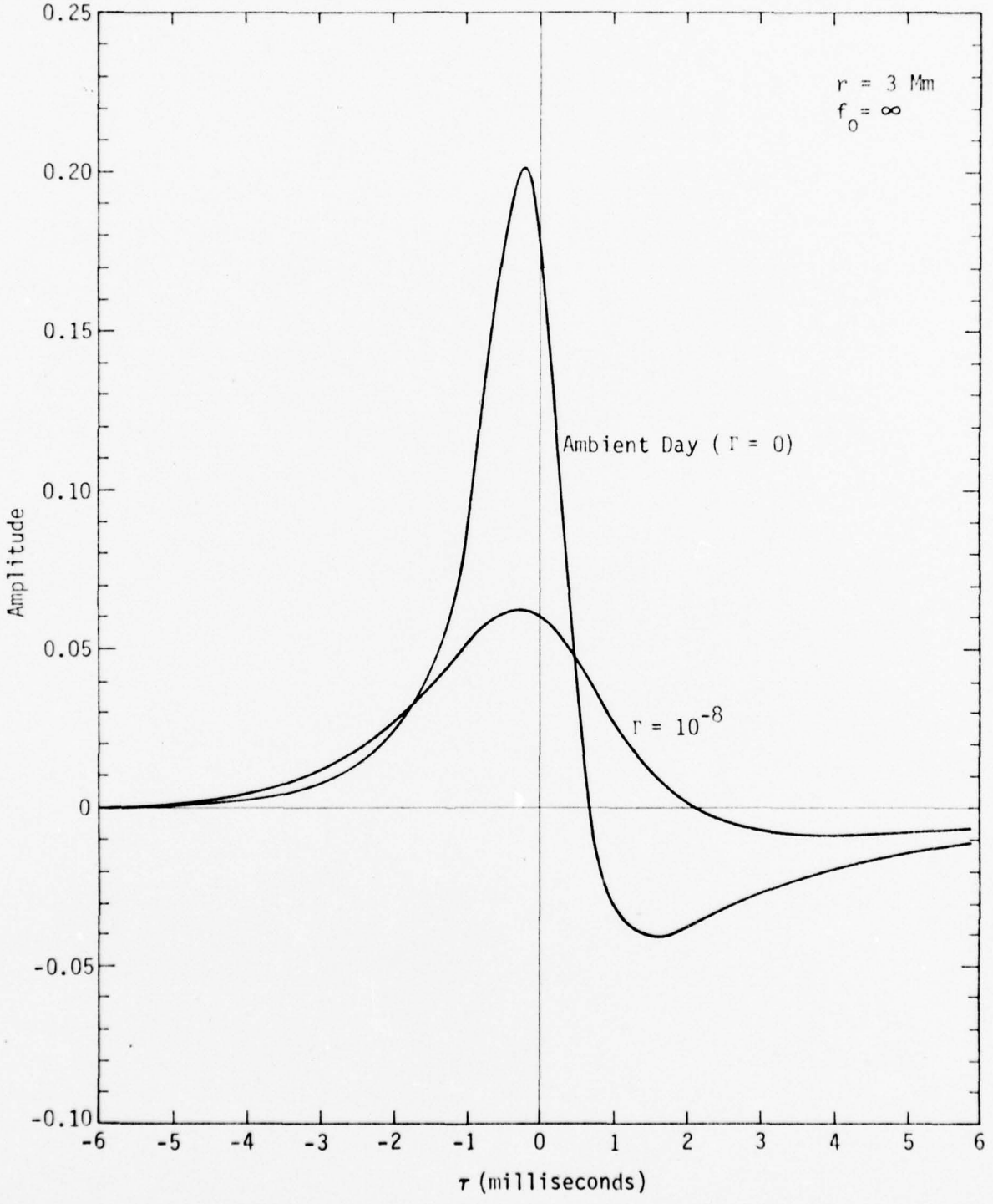

Fig. 6--Calculated ELF electric-field waveform for impulse source: Case B

We next compare the pulse widths in the spread-debris/PCA environment with those for ambient conditions. Again, the results of the comparison depend somewhat on the criterion used for defining the presence or absence of a noise pulse. Fortunately, conclusions on system performance do not depend on the details of the criteria used.

It is immediately evident from Figs. 5 and 6 that the main effect of the disturbed environment is to suppress the peak of the pulse, whereas the tails are nearly unchanged from their ambient characteristics. This behavior is to be expected since the main effect of the disturbed environment is to increase attenuation rate by a factor that is nearly independent of frequency. Since high ELF frequencies are most heavily attenuated under ambient conditions, the absolute increase in attenuation caused by the disturbance is much larger at high frequencies (short times) than at low frequencies (long times). The net result is that the short-duration peak is strongly suppressed relative to ambient, whereas the long-duration pulse tail is not greatly altered.

If a fixed, low threshold is used to define the presence or absence of a noise pulse, then the pulse widths for $\Gamma = 10^{-8}$ are not very different from those for ambient conditions. This behavior occurs because for a fixed, low threshold, the pulse length is defined by the tails, which are not strongly affected by changes in the environment. (See Figs. 5 and 6.) However, if the threshold is defined in terms of peak value, then significant spreading can be attributed to the disturbed environment. This spreading occurs mainly because the peak--and hence the threshold--decreases, whereas the tails remain unaltered, thereby

remaining above the lowered threshold for a longer time. If this type of threshold is used, the factor by which the pulse is lengthened in the nuclear/PCA environment is roughly the same as the factor by which the peak amplitude is reduced. For the cases shown in Figs. 5 and 6, the pulse duration for $\Gamma = 10^{-8}$ is three to four times as long as for $\Gamma = 0$ (ambient) according to this interpretation.

Pulse spreading is of concern in nonlinear noise-processing schemes such as clipping because the fraction of time that the clipper is operative is approximately τ_o/τ_1, where τ_1 is the mean time between pulses. Since clipping "punches holes" in the signal during noise pulses, the ratio τ_o/τ_1 also approximates the fraction of the signal energy lost as a consequence of processing (*Modestino, 1971*). If this ratio is small, the amount of signal lost is much smaller than the amount of noise energy suppressed, and the post-processing SNR will be improved. However, if τ_o/τ_1 becomes nearly unity, then so much signal can be clipped that much of the benefit of nonlinear noise processing is lost. For ambient conditions, τ_1 is typically about 0.1 sec, and τ_o/τ_1 ranges between 0.03 and 0.08 sec depending on conditions, location, definitions, etc. (*Modestino, 1971*). As discussed in Sec. IV, there is no firm reason to expect τ_1 to change much in nuclear environments, except for a very brief period after each burst. Thus, the increase in τ_o/τ_1 is due solely to pulse spreading, which should be no worse than a factor of 3 or 4 greater than ambient. Taking the worst case, τ_o/τ_1 should not exceed about 0.3 (4x0.08) under disturbed conditions, and the resulting signal loss from anomalous spreading would be less than 1.5 dB.

Figures 7 and 8 are analogous to Figs. 5 and 6, and show results for f_o = 300 Hz rather than $f = \infty$. Again, all results are normalized to the waveform labeled "ambient" on Fig. 5. For this realistic receiver bandwidth, the effects of the nuclear/PCA environment on pulse waveform are much less pronounced than for $f_o = \infty$. For example, at r = 1 Mm, the pulse height for $\Gamma = 10^{-8}$ is seen (Fig. 7) to be reduced by only a factor of 2 from its value under ambient conditions, as compared with more than a factor of 3 reduction for $f_o = \infty$ (Fig. 5). These results strengthen our conclusion that, although noise pulses can undergo large anomalous spreading in nuclear/PCA environments, the ratio τ_o/τ_1 does not become large enough to significantly degrade system performance.

PROCESSING GAIN IN DISTURBED ENVIRONMENTS

Figure 4 illustrated how well the two-parameter representation (Eq. (23)) of the APD for ELF noise fitted high-level Saipan noise data. We next show APDs for locations other than Saipan and for disturbed conditions, and give results showing the effect of changes in environment/location on desired clip level.

First, consider the effect of a spread-debris nuclear (or a PCA) environment on the APD. As discussed in Sec. II, the noise (and signal) excitation factor would probably increase by up to a few decibels due to the lowering of ionospheric reflection heights. In addition, the attenuation of ELF waves propagating in the earth-ionosphere waveguide can increase by as much as 1 or 2 dB/megameter (depending on frequency) over the attenuation experienced under ambient conditions. Since the Gaussian component of the noise propagates over greater distances than

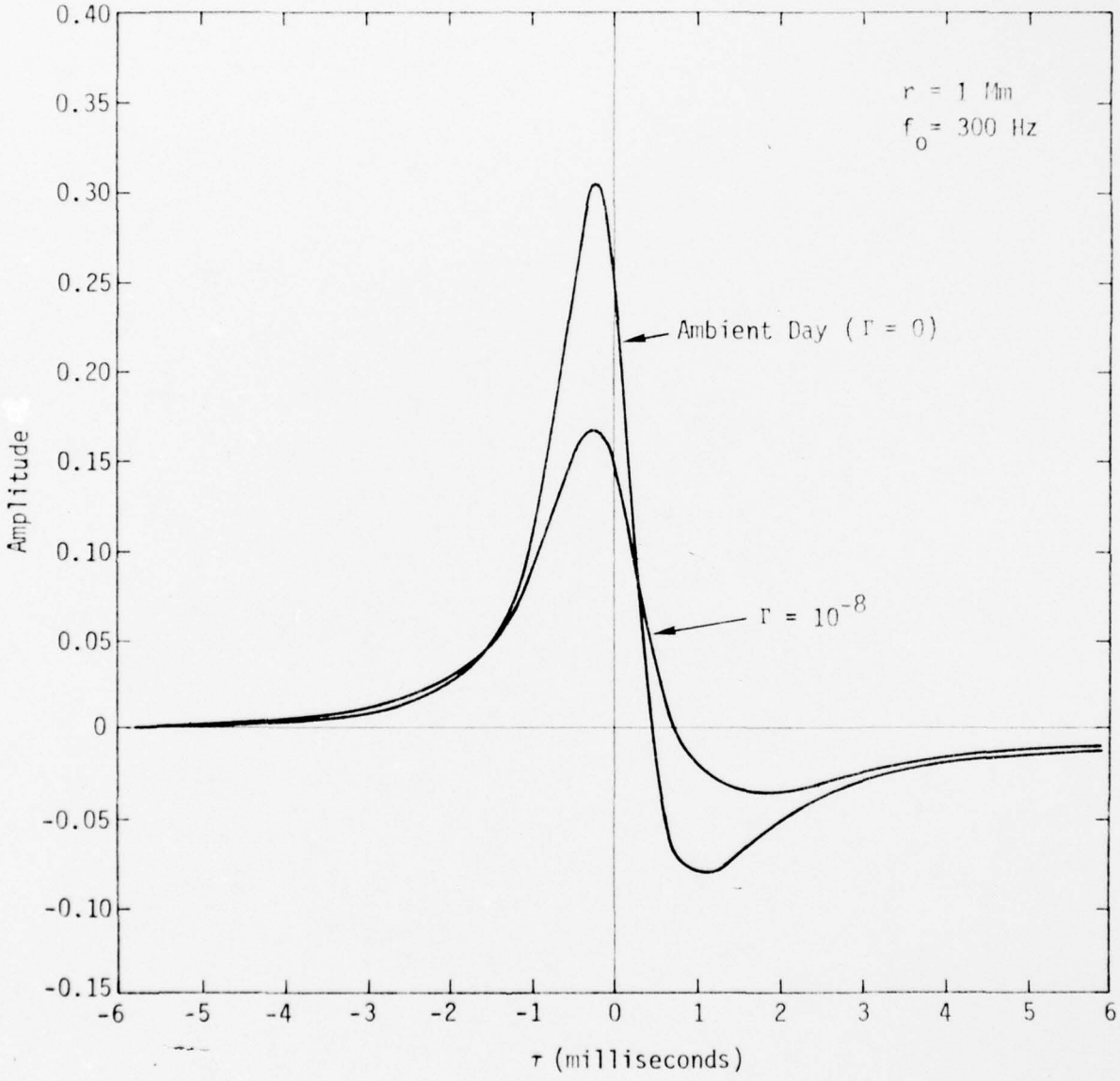

Fig. 7--Calculated ELF electric-field waveform for impulse source: Case C

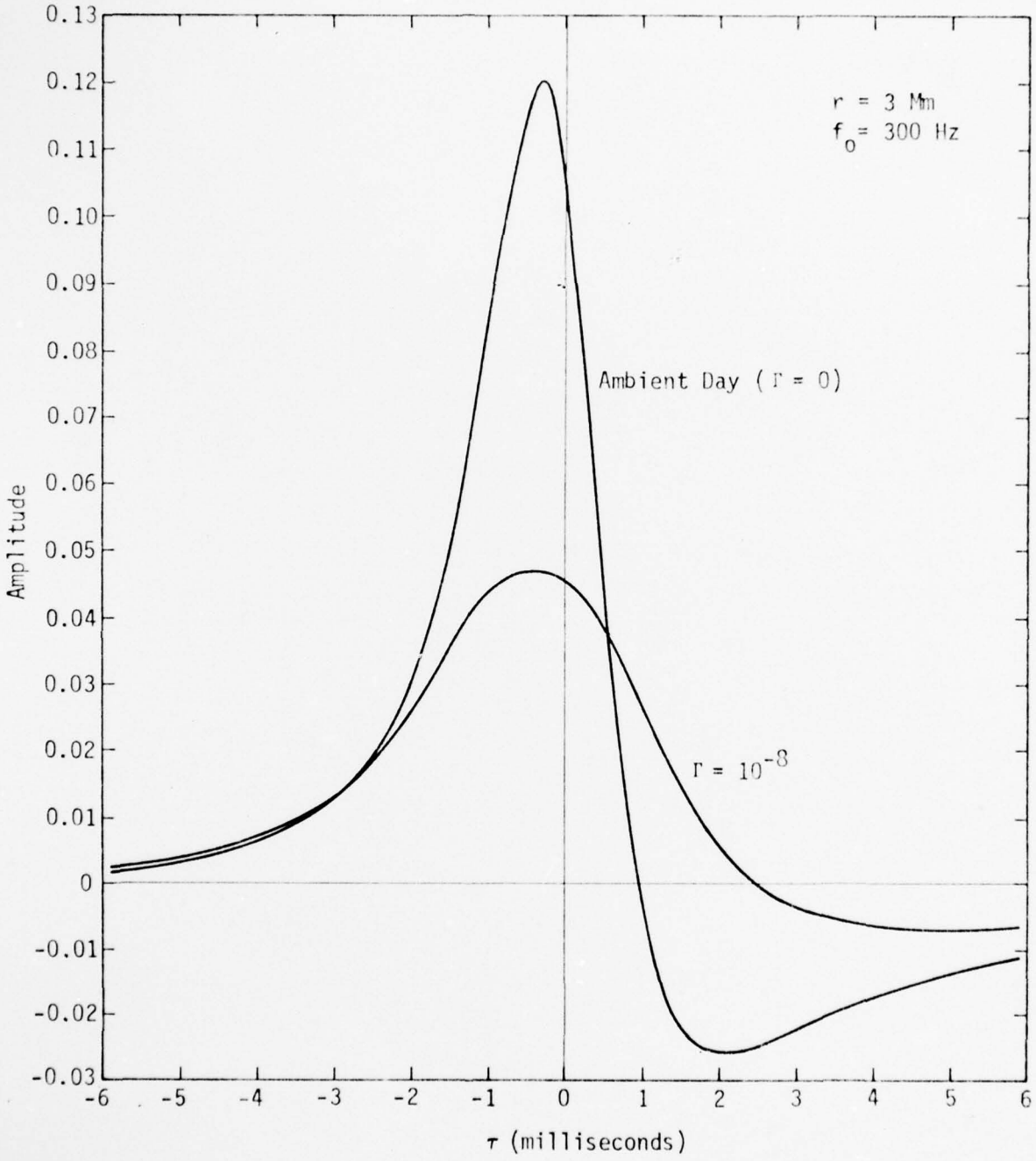

Fig. 8--Calculated ELF electric-field waveform for impulse source: Case D

the Rayleigh (spikey) component, the net effect of a spread-debris environment is to reduce the relative importance of the Gaussian component; i.e., the spread-debris environment causes γ to increase over its ambient value.

Of course, the spread-debris model is highly idealized. For more complex environments that exhibit pronounced lateral inhomogeneities, the net effect on the APD is a strong function of the relative locations of the disturbance, nearby thunderstorm activity, distant thunderstorm activity, and the receiver. For example, a disturbance localized over lightning activity far from the receiver could cause a slight *increase* in the relative importance of the Gaussian component, as could a disturbance localized between nearby activity and the receiver. Moreover, the change in SNR caused by environmental changes depends on the location of the transmitter in addition to the parameters given above. However, the spread-debris model illustrates the type of changes to be expected in the APD and optimum clip levels. A processing scheme designed to perform well for a variety of spread-debris environments should perform well in other environments that, although more complex to analyze, would not distort the APD any more severely.

Figure 9 shows the manner in which the high-level Saipan APD can be altered by widespread ionospheric disturbances. In addition to the ambient APD, which corresponds to $\gamma = 4.4$ (13 dB), results for two disturbed cases are shown. One of these cases corresponds to a "moderate" change in APD resulting from the Gaussian component being decreased 5.5 dB relative to the Rayleigh component; i.e., γ increases from its ambient value of 4.4 (13 dB) to 8.4 (18.5 dB). This level

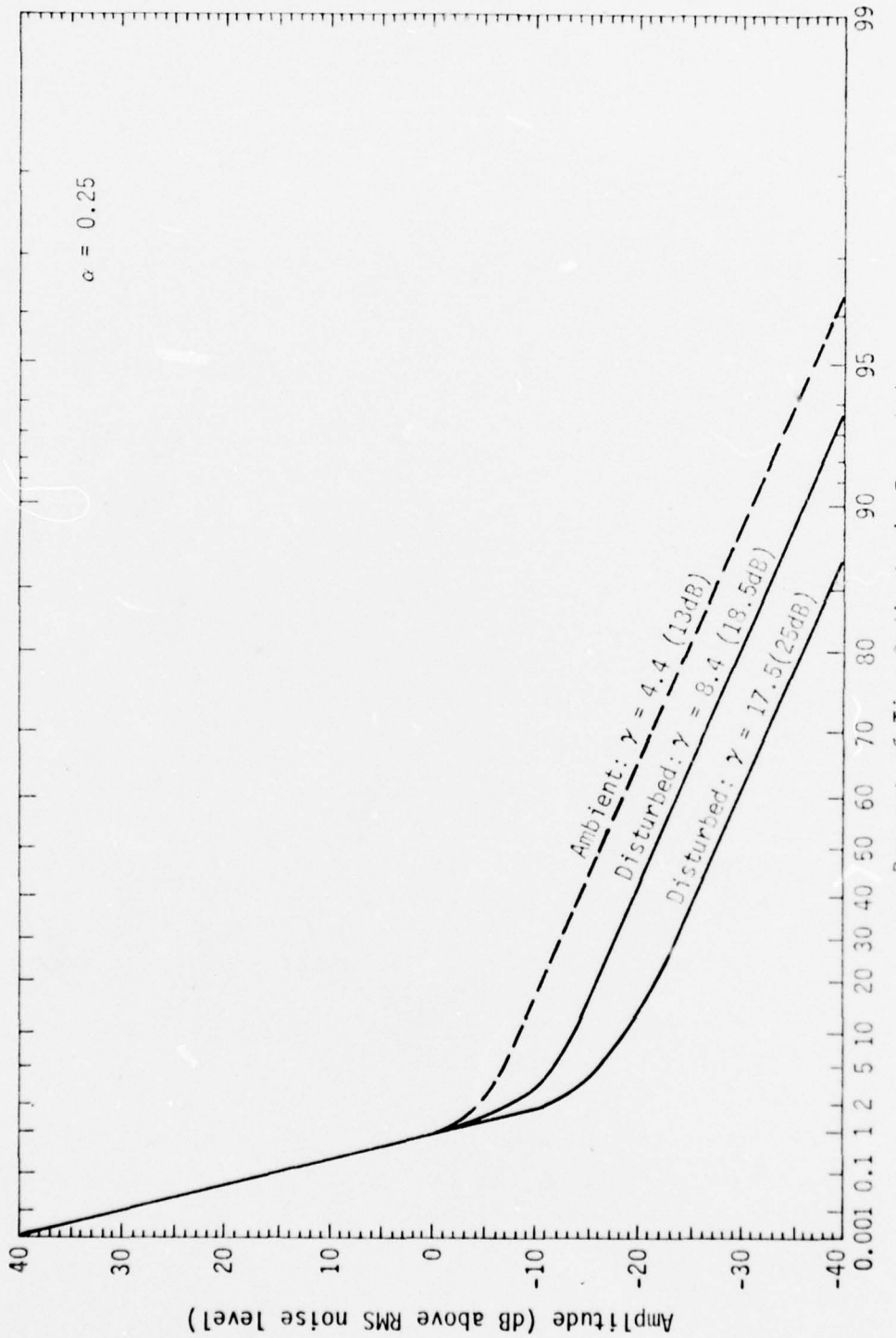

Fig. 9--APD of high-level Saipan ELF noise in ambient and disturbed environments.

of change is quite reasonable and, for example, corresponds to a 1.1-dB/megameter increase in attenuation rate (averaged over the receiver bandwidth) in a situation where the sources of Gaussian noise are 5 Mm farther from the receiver than are the sources of Rayleigh noise. The other case shown is extreme, and corresponds to the Gaussian component being decreased 12 dB (γ increases from 4.4 to 17.5) relative to the spikey component. This level of change might correspond, for example, to a 2-dB/megameter increase in attenuation rate and a 6-Mm difference in propagation path length.

It is important to note that, although the *ratio* of Gaussian to non-Gaussian noise can diminish markedly--5.5 dB and 12 dB for the cases considered here--the change in *total* RMS noise can be quite small. This behavior occurs because total RMS noise is dominated by impulses from nearby lightning flashes that, due to the relatively short propagation path, do not suffer large loss of energy in disturbed environments. The main effect is usually a reduction in the Gaussian noise, which does not greatly affect total RMS noise; i.e., significant reductions in σ_o^2 do not greatly affect the sum $R_o^2\Gamma(1 + \frac{2}{\alpha}) + \sigma_o^2$. It follows that clip levels should be based on the ratio, γ^2, of Gaussian to non-Gaussian noise rather than on total RMS noise.

Figure 10 shows processing gain (Eq. (27)) as a function of clip level (in RMS units) for high-level Saipan noise. For example, for ambient conditions, setting the clip level 20 dB above RMS provides a processing gain of 4 dB, whereas a setting of -13 dB gives the maximum achievable gain of 13 dB. For this case, lower settings are not desirable. No additional processing gain can be achieved since the

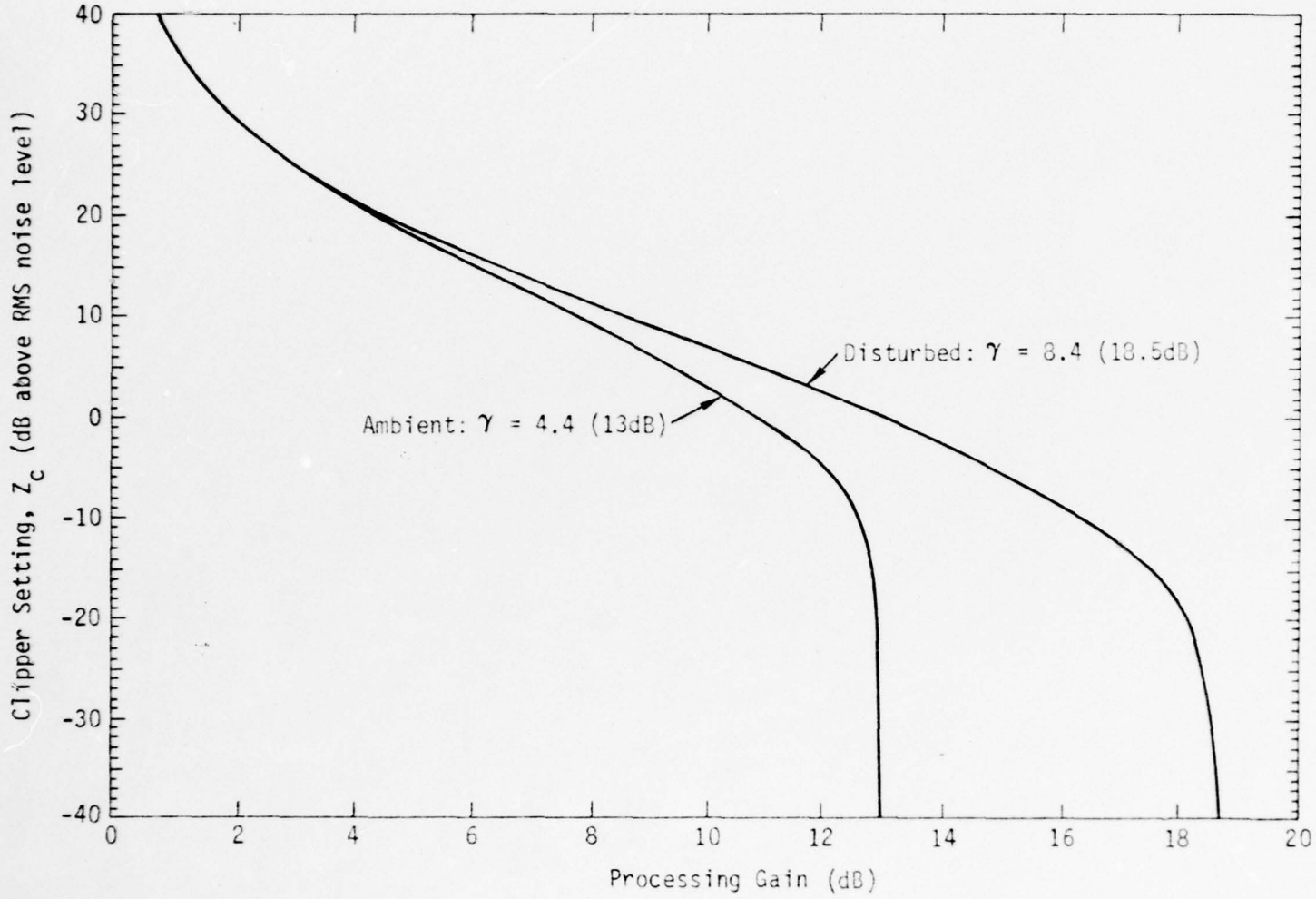

Fig. 10--Processing gain versus clipping level for high-level Saipan ELF noise

spikey component is only 13 dB above the Gaussian component, and lower settings would degrade any signal that might be present. For the disturbed case, Fig. 10 shows that setting the clip level at -15 to -20 dB gives the maximum gain of 10 Log $[1+(8.4)^2]$ = 18.5 dB.

To assess the expected performance of ELF noise processors, Figs. 9 and 10 must be used together. An experimental ELF noise clipper, developed as part of the SANGUINE system, continuously adapts so that clipping occurs some specified fraction of the time (*Bernstein, et al., 1974*). The precise value of this fraction is not critical, but 40 to 60 percent proved successful for ambient noise. For ambient conditions, Fig. 9 shows that clipping occurs 40 percent of the time if the clip level is set at -13 dB and 60 percent of the time if the level is set at -17 dB. From Fig. 10, it is seen that either setting gives essentially the maximum achievable (13 dB) processing gain. Moreover, a clip level as high as -10 dB, which corresponds to clipping 20 percent of the time for ambient high-level Saipan noise (Fig. 9), also gives about 13 dB of processing gain. Thus, within reasonable bounds, the predicted processing gain is not a sensitive function of clip level.

For the moderately disturbed case shown in Fig. 9 (γ = 8.4), clipping occurs 20 and 60 percent of the time if the clip level is set at -15 and -23 dB, respectively. Figure 10 shows that, in either case, the maximum processing gain of 18.5 dB is approached. These results suggest a rule of thumb that is perhaps evident on intuitive grounds. Specifically, if the clip level is set so that clipping occurs a fraction of the time corresponding to the Gaussian region of an APD graph, nearly optimum noise suppression results. More

simply, for the type of APD plot shown on Fig. 9, the clip level should be set a few decibels below the knee in the curve.

APDs and corresponding processing gains versus clip levels are shown for moderate-level Malta noise and Norway noise in Figs. 11 through 14. These results reinforce the main conclusions drawn above: (1) Pacific-Sierra's model agrees well with measured APDs, and (2) *a single clipping fraction in the 20- to 60-percent range gives about the optimum processing gain in both nuclear and ambient environments.* The design of the experimental SANGUINE clipper thus appears well suited to a wide range of environmental conditions.

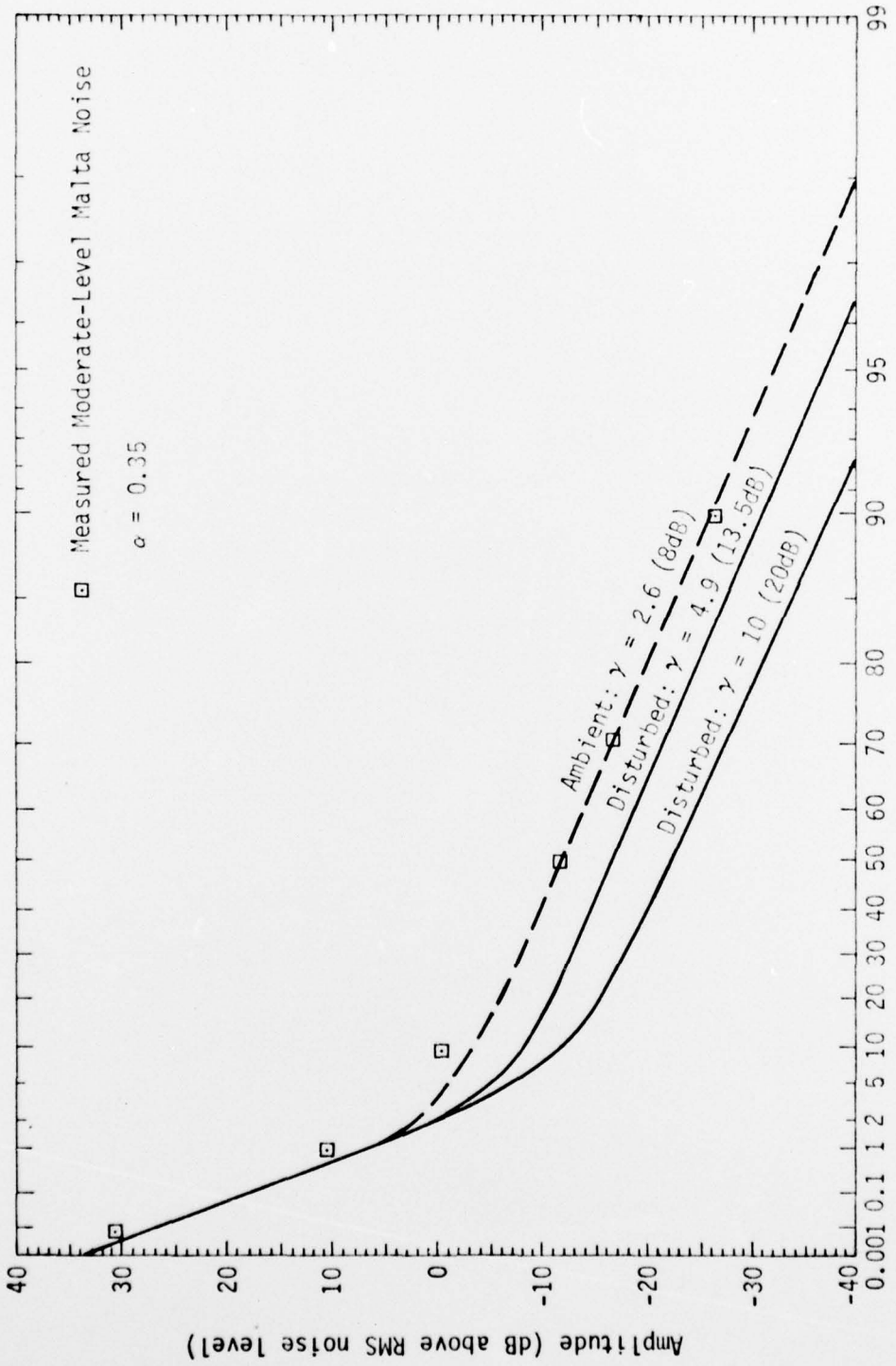

Fig. 11--APD of moderate-level Malta ELF noise in ambient and disturbed environments

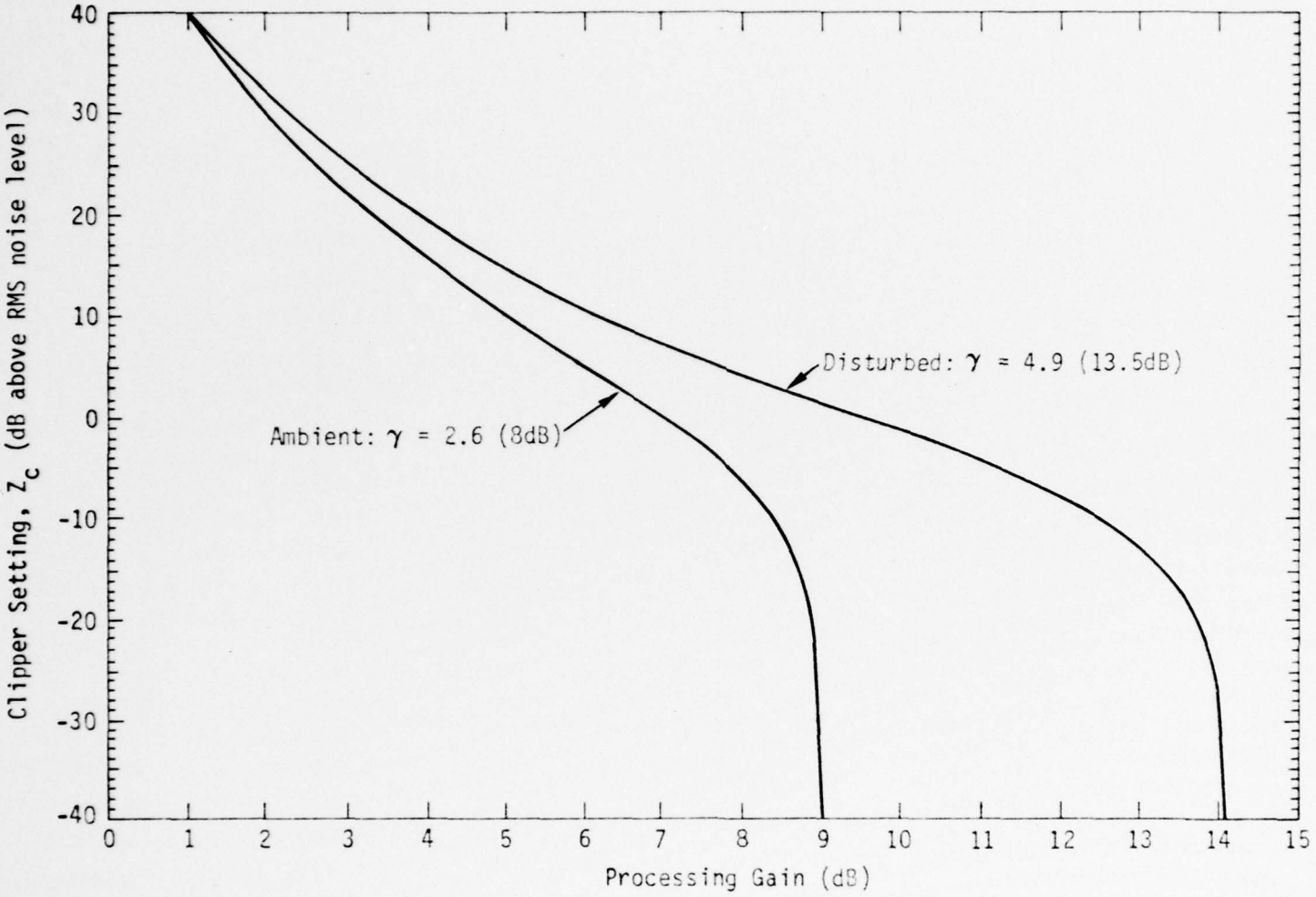

Fig. 12--Processing gain versus clipping level for moderate-level Malta ELF noise

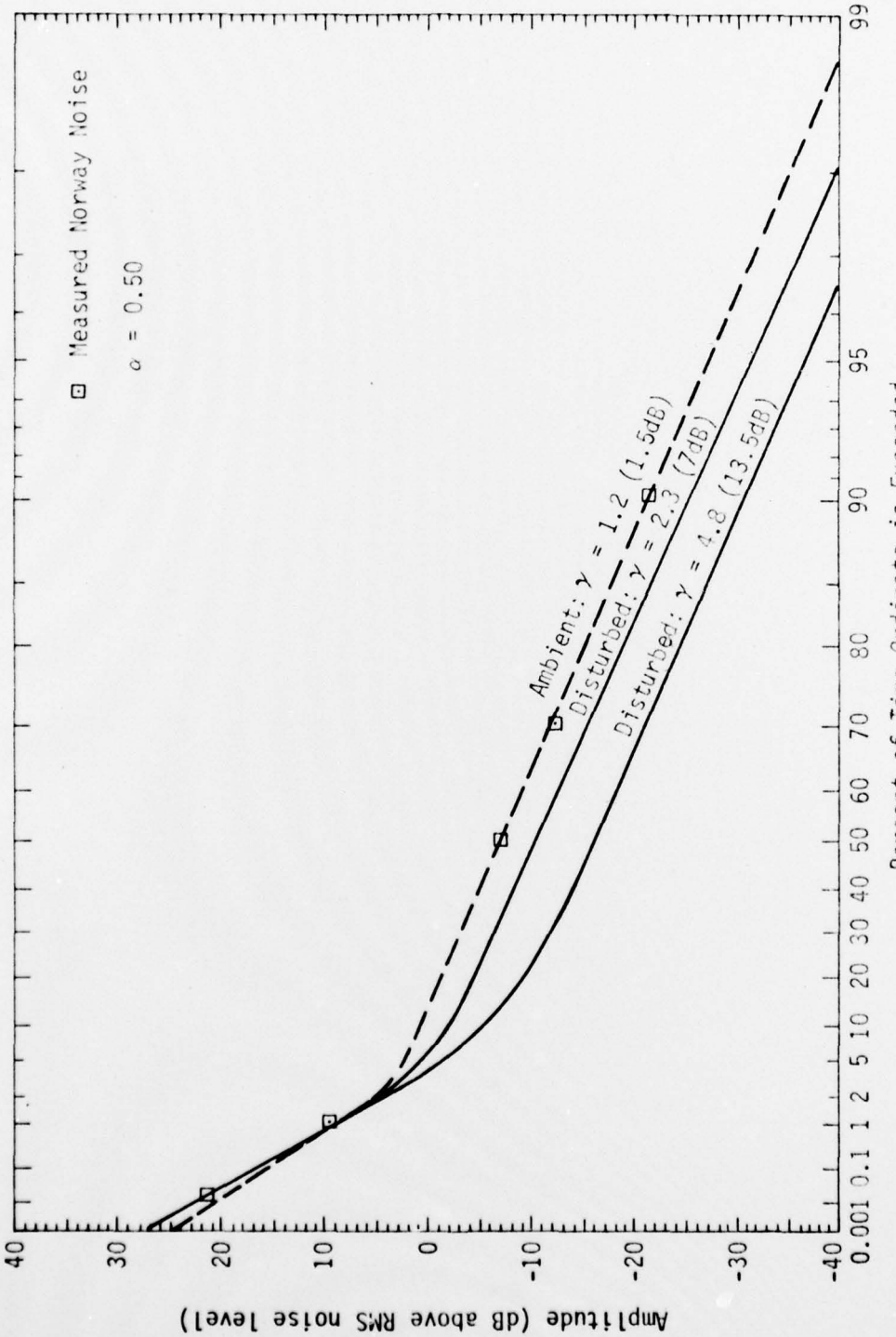

Fig. 13--APD of Norway ELF noise in ambient and disturbed environments

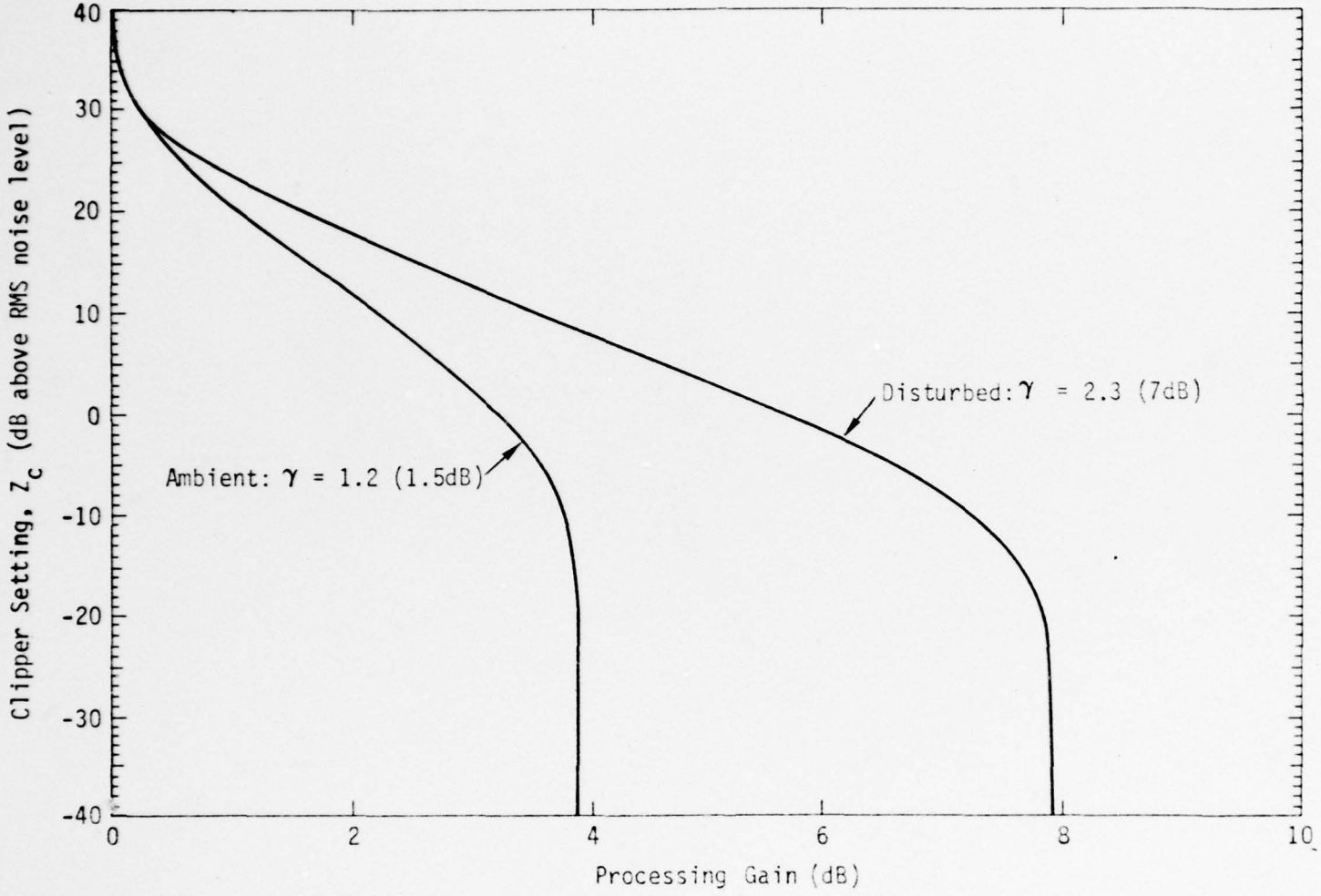

Fig. 14--Processing gain versus clipping level for Norway ELF noise

IV. LIGHTNING ACTIVITY UNDER POST-DETONATION CONDITIONS

Previous sections have been concerned primarily with the effects of anomalous propagation on ELF noise statistics and noise-pulse durations. However, other mechanisms exist that could act as sources of atmospheric noise in nuclear environments. The most obvious mechanism is the electromagnetic pulse (EMP), which is lightning-like. Moreover, lightning flashes have been induced by ground-level nuclear bursts, including a thermonuclear detonation at Eniwetok Atoll (*Uman, et al., 1972*). These induced flashes were distinct from the EMP, and were apparently caused by charge and electric fields generated by Compton electrons produced by gamma radiation from the detonation. The time duration of the observed flashes was less than 100 msec. Thus, for a small fraction of a second after a nuclear burst, an EMP possibly followed by induced lightning will increase the atmospheric noise. However, such a short-lived increase in noise should not seriously degrade ELF communication system performance.

In principle, surface heating from widespread fires started as a result of a nuclear conflict could produce thunderstorm lightning by triggering convective instability. If such a phenomenon indeed occurred, an increase in ELF atmospheric noise persisting for hours could result. Accordingly, as part of the study reported herein, a small amount of effort was expended to determine whether any evidence existed that large-scale fires could induce lightning activity. Because an analytic treatment would be intractable, the approach taken was to contact authorities and survey literature on forest fires. As might be expected, the results of the survey were somewhat inconclusive due to a lack of

hard data. Most of the people contacted felt that the available data in no way indicated that large fires induced lightning. This conclusion was based on the observation of numerous fires with no associated lightning.† Of course, these observations could be misleading because forest fires usually occur in hot dry weather not conducive to lightning activity. In one instance--the Pelican Fire in the El Dorado National Forest--three and one-half hours of thunderstorms ensued. There is no way to ascertain whether these storms would have occurred in the absence of the fire.

The most detailed discussion of meteorological conditions before, during, and after a large fire is presented by Bond, *et al. (1967)* in reporting on the huge brushfires in southeastern Tasmania on 7 February 1967. It was concluded that some large convective clouds were triggered by the fires and that, before the fires, the air mass exhibited considerable instability. Thus, there exists tenuous evidence that widespread fires could stimulate thunderstorm activity provided that pre-existing conditions are suitable.

On the basis of the above information, it is our preliminary conclusion that thunderstorm activity will not increase significantly--say, an order of magnitude--in the post-detonation environment. Obviously, a great deal of uncertainty is associated with this conclusion.

---

†For example, one member of the U.S. Forest Service, Northern Forest Fire Laboratory, stated that in 20 years of observing forest fires, some of them enormous, he had not once detected lightning.

V. CONCLUSIONS

Analytic expressions that describe ELF noise-pulse waveforms and noise APDs have been derived. In both cases good agreement is obtained with available experimental data and with results from much more complicated numerical treatments. Moreover, these expressions, which depend explicitly on readily calculated parameters, such as attenuation rate in the earth-ionosphere waveguide, are particularly convenient for predicting changes in noise characteristics caused by nuclear/PCA environments.

It was found that, depending on certain definitions, noise-pulse durations could increase by as much as a factor of three or four in nuclear/PCA environments. Most of this anomalous pulse spreading is caused by increased attenuation, which selectively removes highest-frequency Fourier components from the ELF noise-pulse. The maximum loss in processing gain caused by anomalous pulse spreading was found to be no greater than 1 or 2 dB. *Smearing of noise pulses in disturbed environments therefore does not pose a major problem to nonlinear noise suppression in ELF communication systems.*

A major effect of the ionospheric disturbances considered was a significant increase in the ratio of the energy carried in noise spikes to the energy of the background Gaussian noise component. This change in ratio, which altered the APD considerably, occurred because Gaussian noise tends to be suppressed relative to noise spikes by the increased attenuation typically associated with nuclear/PCA environments. However, total RMS noise, to which noise spikes make the major contribution, might well change only slightly. Consequently, to achieve maximum processing gain,

clip levels should be set according to the ratio of noise-spike energy to Gaussian-background energy.

Because this ratio can change drastically, an adaptive procedure is called for. *Calculations show that the experimental SANGUINE noise-suppression circuit that self-adapts to clip some specified fraction--typically 20 to 60 percent--of the time gives nearly optimum processing gain for a wide variety of ambient and nuclear/PCA environments.*

REFERENCES

Abramowitz, M., and I.A. Stegun, *Handbook of Mathematical Functions*, Nat. Bur. Standards Appl. Math. Series 55, U.S. Govt. Printing Office, June 1964.

Bernstein, *et al*, "A Signaling Scheme and Experimental Receiver for Extremely-Low-Frequency (ELF) Communications," *IEEE Trans. on Communication*, *COM-22*, April 1974, p. 508.

Bond, H.E., *et al*, *Report on the Meteorological Aspects of the Catastrophic Bushfires in South Eastern Tasmania on 7 February 1967*, Commonwealth of Australia, Director of Meteorology, Melbourne, November 1967.

Budden, K.G., *The Waveguide Mode Theory of Wave Propagation*, Logos Press, London, 1967.

Crain, C.M., "A Note on Persisting Radio Propagation Effects After High-Altitude Nuclear Bursts," *J. Geophys. Res.*, *68*, November 1, 1964, p. 4717.

Erdélyi, A., *Tables of Integral Transforms*, *Vol. 1*, McGraw-Hill Book Co., New York, 1954.

Evans, J.E., and A.S. Griffiths, "Design of a Sanguine Noise Processer Based Upon World-Wide Extremely Low Frequency (ELF) Recordings," *IEEE Trans. on Communications*, *COM-22*, April 1974, p. 528.

Field, E.C., "Propagation of ELF Waves Under Normal and Naturally Disturbed Conditions," *J. Geophys. Res.*, *74*, July 1, 1969, p. 3639.

Fischer, P.G., and W.S. Knapp, *Aids for the Study of Electromagnetic Blackout*, General Electric Company, TEMPO, DASA 1923, Santa Barbara, California, March 1967.

Galejs, J., *Terrestrial Propagation of Long Electromagnetic Waves*, Pergamon, New York, 1972.

Griffiths, A.S., *ELF Noise Processing*, Lincoln Laboratory, Tech. Rept. 490, January 13, 1972.

Jones, D.L., "Propagation of ELF Pulses in the Earth-Ionosphere Cavity," *RADIO SCIENCE*, *Vol. 5*, August-September 1970, p. 1153.

Modestino, T.W., *A Model for ELF Noise*, Lincoln Laboratory, Tech. Rept. 493, December 16, 1971.

Uman, M.A., *et al*, "Lightning Induced by Thermonuclear Detonation," *J. Geophys. Res.*, *Vol. 77*, March 20, 1972, p. 159.

Wait, T.R., *Electromagnetic Waves in Stratified Media*, The MacMillan Co., New York, 1962.

DISTRIBUTION

Director
Field Projects, Earth Sciences Division
Office of Naval Research
Department of the Navy
800 North Quincy Street
Arlington, Virginia 22217

Office of Naval Research
1030 East Green Street
Pasadena, California 91106

Commander
Defense Contract Administration Services Region
11099 South La Cienega Boulevard
Los Angeles, California 90045

Director
U.S. Naval Research Laboratory
Washington, D.C. 20390
Attention: Code 2629
Code 2627

Defense Documentation Center
Cameron Station
Building 5
Alexandria, Virginia 22314

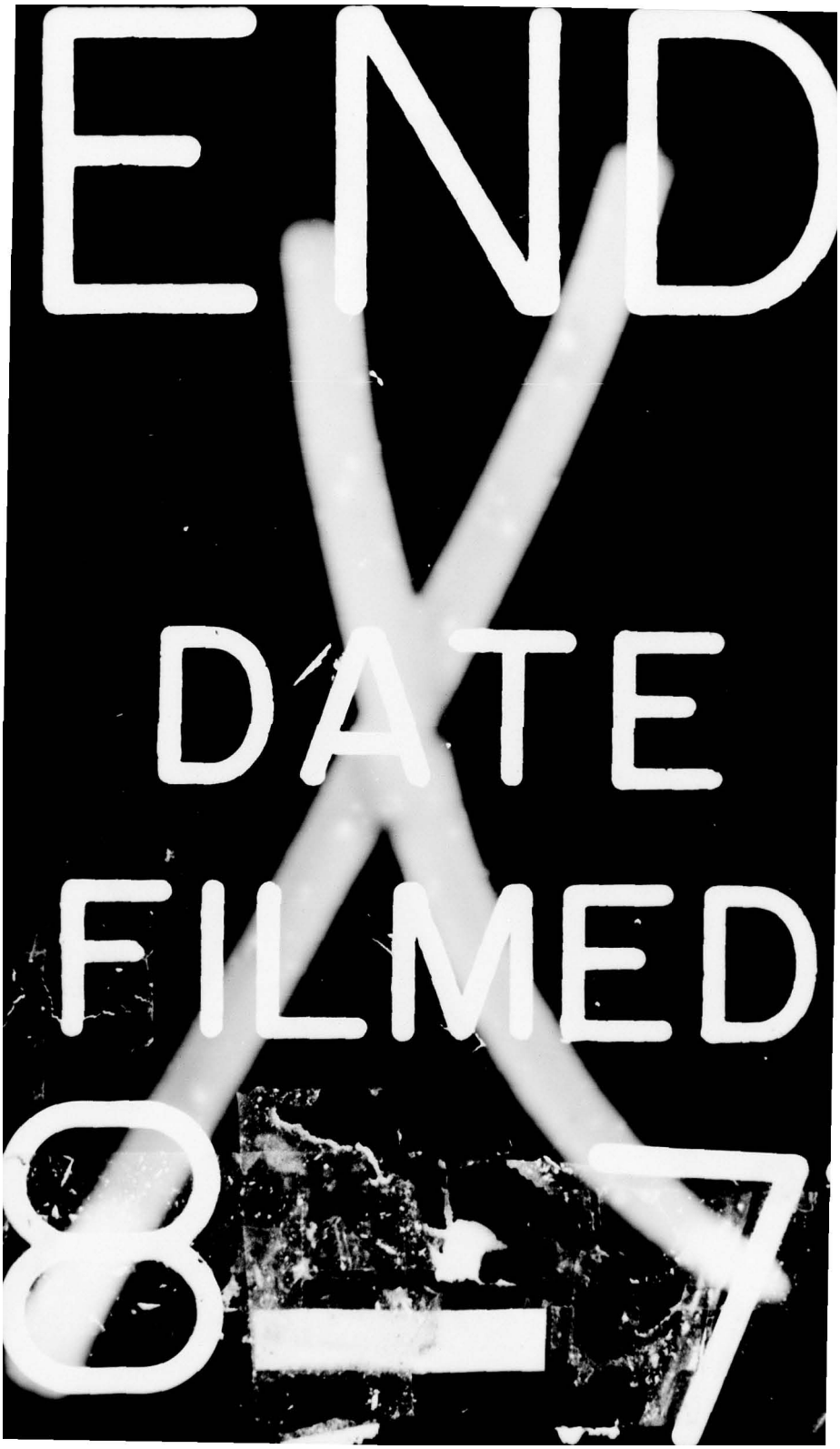
END
DATE
FILMED
8-87

D-A042 116 ELF NOISE STATISTICS AND PROCESSING UNDER DISTURBED CONDITIONS(U) PACIFIC-SIERRA RESEARCH CORP SANTA MONICA CALIF E C FIELD ET AL. DEC 74 PSR-411 N00014-74-C-0234

2/2

NCLASSIFIED F/G 9/3 NL

SUPPLEMENTARY

INFORMATION

Errata

AD-A042 116

Pages iv, viii, and 46 are blanks.

DTIC-DDAC
30 Aug 84